NASA CONTRACTOR REPORT

NASA CR-340

THE MAXIMUM RESPONSE OF A LINEAR MECHANICAL OSCILLATOR TO STATIONARY AND NONSTATIONARY RANDOM EXCITATION

by R. L. Barnoski

Prepared under Contract No. NAS 5-4590 *by*
MEASUREMENT ANALYSIS CORPORATION
Los Angeles, Calif.
for Goddard Space Flight Center

NATIONAL AERONAUTICS AND SPACE ADMINISTRATION - WASHINGTON, D. C. - DECEMBER 1965

NASA CR-340

THE MAXIMUM RESPONSE OF A LINEAR MECHANICAL OSCILLATOR TO STATIONARY AND NONSTATIONARY RANDOM EXCITATION

By R. L. Barnoski

Prepared under Contract No. NAS 5-4590 by
MEASUREMENT ANALYSIS CORPORATION
Los Angeles, Calif.

for Goddard Space Flight Center

NATIONAL AERONAUTICS AND SPACE ADMINISTRATION

For sale by the Clearinghouse for Federal Scientific and Technical Information
Springfield, Virginia 22151 – Price $3.00

ABSTRACT

This report considers the peak response behavior of a mass excited, linear mechanical oscillator when the applied random excitation is either stationary or nonstationary. The stationary random excitation is Gaussian bandwidth limited white noise and the nonstationary random excitation is Gaussian bandwidth limited white noise shaped in time by (1) a rectangular envelope function or (2) a half-sine envelope function. Thus, the nonstationary excitation appears as a pulse of white noise shaped as either a rectangle or a half-sine.

Using data from an analog computer study, two topics are explored in detail.

- the expected maximum peak response in a finite time interval for a specified probability of occurrence
- a measure of the time duration for the oscillator to achieve stationarity in its response

The peak response is expressed as parametric, dimensionless plots of the peak to rms response ratio and a dimensionless time parameter. In this form, the oscillator response to stationary white noise and to the pulsed random excitation can be conveniently compared and can be used to estimate directly the time duration for an oscillator to achieve stationarity in its response. It is found that for values of the dimensionless time parameter greater than about one, the stationary results can be applied to conservatively predict the oscillator peak response to the pulsed excitation.

For both stationary and nonstationary excitations, the peak behavior is noted to be dependent on the oscillator damping for a small number of response cycles. As the number of response cycles becomes large, the peak to rms response behavior tends to become independent of damping.

TABLE OF CONTENTS

LIST OF FIGURES

LIST OF FIGURES (continued)

LIST OF SYMBOLS

B	noise bandwidth
B_r	half-power bandwidth
$C_{xx}[\ ]$	covariance function in [ ]
$C_{xy}[\ ]$	cross-covariance function in [ ]
c	viscous damping coefficient
$E[\ ]$	mean value of [ ] averaged over an ensemble of records
$E(t)$	envelope function in time
f_n	undamped natural frequency of the oscillator in cycles per second
$f(t)$	functional notation for a random excitation
$G_0(f)$	magnitude of the white noise input excitation
$G_\alpha(\omega_n)$	magnitude of the one-sided power spectrum at the frequency ω_n
$H[\omega]$	frequency response function for a linear system
$h(\tau)$	impulse response of a linear system
i	complex operator = $\sqrt{-1}$
k	linear spring constant of the mechanical oscillator
m	mass of the mechanical oscillator
$P_M(\ )$	probability that M, the maximum value obtained, is $\leq$ ( ) times the rms value
$P_E(\ )$	probability that an individual envelope peak is $\leq$ ( ) times the rms value
Q	measure of damping of the oscillator
$R_{xx}[\ ]$	autocorrelation function in [ ]
$R_{xy}[\ ]$	cross-correlation function in [ ]
$S_{xx}[\ ]$	two-sided power spectral density function in [ ]
$S_{xy}[\ ]$	two-sided cross spectra in [ ]
T	elapsed time for observing the system response to white noise
T^*	dimensionless time parameter
x	displacement from static equilibrium for the mechanical oscillator
$\dot{x}$	velocity of the mechanical oscillator
$\ddot{x}$	acceleration of the mechanical oscillator

LIST OF SYMBOLS (Continued)

$Z[\ ]$	mechanical impedance of the structure
$\alpha(t)$	random acceleration function
β	peak to rms response ratio for the response of the single degree-of-freedom system
$\Delta\tau$	effective time duration of the pulsed excitation
ζ	damping ratio for the single degree-of-freedom system
λ	bandwidth of the filter
$\mu[\ ]$	the mean value of $[\ ]$
μ_n	average number of envelope peaks per second
$\mu_n T$	average number of envelope peaks that occur during time T
$\sigma^2[\ ]$	variance in $[\ ]$
$\psi^2(\ )$	mean square value
ω	excitation frequency
ω_d	damped natural frequency of the system
ω_n	undamped natural frequency for the single degree-of-freedom system
$[\ ]$	time average of $[\ ]$

THE MECHANICAL RESPONSE OF A LINEAR MECHANICAL OSCILLATOR TO STATIONARY AND NONSTATIONARY RANDOM EXCITATION

1. INTRODUCTION

This report treats the response behavior of a linear, time invariant mechanical oscillator subjected to Gaussian random excitation. For these conditions, the response is random in nature and is characterized by Gaussian properties. As such, only the first two statistical moments are required to provide the probabilistic description of the random response. The complexity of the statistical moments, however, depends upon whether the random excitation is stationary or nonstationary, whether the system is unimodal or multimodal, and whether the transient response of the system is included or ignored.

The classic unimodal system is the mechanical oscillator (also commonly referred to as a single degree-of-freedom mechanical system) whereas the multimodal system implies a distributed elastic structure. The distributed structure generally requires attention be given to space-time correlation of the random loading whereas the mechanical oscillator requires only correlation in time. Including transient conditions in a solution introduces nonstationarity into the response for the initial intervals of time.

Reports dealing with response properties categorically include the mean value, mean square response, correlation functions and power spectra. This report, however, comments only in passing on these properties and emphasizes the peak response behavior of the oscillator when the applied excitation is (1) stationary and (2) nonstationary.

The output response to stationary Gaussian random excitation of a lightly damped, linear mechanical oscillator appears as sketched in Figure 1. The output is Gaussian and appears like a sinusoid at frequency f_n with a slowly varying random amplitude and random phase. The amplitude of the response is shown as enveloped in time so that it becomes proper to speak of the statistical properties of the envelope as well as the response time history. The

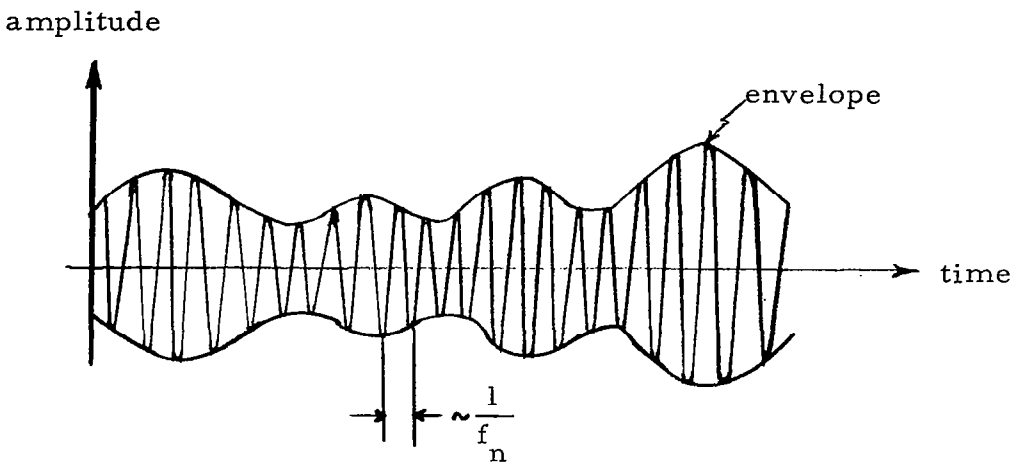

Figure 1. Response of a Lightly Damped Mechanical Oscillator to Broadband Stationary Random Excitation

instantaneous probability density for the amplitude of the response time history is Gaussian. The probability density is nearly Rayleigh for the distribution of the peaks of the response time history. As the oscillator damping approaches zero, the probability density of the peaks of the time history approaches a Rayleigh distribution. In the limit, that is, when the oscillator damping becomes infinitesimally small thus defining an infinitely narrow bandpass filter, the peaks of the response time history are distributed according to the Rayleigh distribution. The probability density for the envelope maxima obtained by passing white noise through an ideal bandpass filter is given by Rice on page 223 of Reference 1. Although resembling the Rayleigh distribution, the envelope maxima density is noted to appear as neither Rayleigh nor Gaussian. Even though these properties and other such relationships (Reference 2) are known for simple linear systems and stationary random excitation, several important questions still cannot be answered.

One such question is, "What is the probability of exceeding a stated amplitude within a finite period of time?" Expresses in an alternate manner, "For a stated probability, how large an amplitude will occur (on the average)

within a finite period of time?" To answer this question demands a time dependent probability whose analytical expression still remains unknown at this writing. The solution, however, finds immediate application in the mechanical design of missiles and spacecraft. Since exposure to maximum levels of random excitation occurs for short time periods (for example, at launch, near Mach 1, or at maximum Q in the flight profile), it may be possible to save considerable weight by establishing structural reliability criteria based on a time related probability of extreme loads.

Another related question is, "What is the time duration for a mechanical oscillator to achieve stationarity in its response to impulsively applied random excitation?" If the nonstationary excitation is white noise enveloped in time by the unit step function, the response will not be stationary for the initial intervals of time. After some finite time duration, however, the oscillator response exhibits stationary characteristics and the results from stationary analyses then can be applied. If the nonstationary excitation is white noise enveloped in time by a rectangular or half-sine pulse, the response characteristics become somewhat more difficult to codify. A solution for this problem finds application in the design of systems subjected to random shock loadings.

Answers to these questions based on the peak response of a linear oscillator require knowledge of the distribution of the response maxima in time. Specifically, it is required to know the distribution of time between level crossings or, alternatively, the distribution of time intervals between peaks above a stated level. This is an extremely difficult problem and no general analytical solution is available at this time for these time dependent distributions. Thus, it becomes appropriate to make rather sweeping simplifying assumptions so that an approximate time dependent distribution can be written for the response maxima. The main portion of this report traces the analytical development of one such "approximate" time dependent distribution and compares predicted analytical results with empirical data from an analog computer study.

2. STATISTICAL PROPERTIES

Although the statistical properties of a Gaussian random process are discussed elsewhere, it is instructive to briefly consider here the definitions of those functions which are alluded to in this report. The statistical quantities of interest are the mean, the variance, and the covariance functions. These are defined for stationary and nonstationary random processes.

2.1 STATIONARY AND ERGODIC CONDITIONS

Consider the statistical moments of a stationary ergodic random process x(t). The assumption of ergodicity allows one to calculate the statistical properties of the random process by time averaging a single record from the random process. The first order statistical moment is the mean μ and is defined as

$$\mu = E[x(t)] = \overline{x} = \lim_{T\to\infty} \frac{1}{T} \int_0^T x(t)\, dt \tag{2.1}$$

A second order statistical moment is the autocorrelation function $R_{xx}(\tau)$ and is defined as

$$R_{xx}(\tau) = E[\, x(t)\, x(t+\tau)\,] \tag{2.2}$$

For $\tau = 0$, the autocorrelation function reduces to the mean square value ψ^2 which may be written as

$$R_{xx}(0) = \psi^2 = E[\, x^2(t)\,] = \overline{x^2} = \lim_{T\to\infty} \frac{1}{T} \int_0^T x^2(t)\, dt \tag{2.3}$$

The covariance function $C_{xx}(\tau)$ also is a second order statistical moment and appears as

$$C_{xx}(\tau) = E\left\{[\, x(t) - \mu\,][\, x(t+\tau) - \mu]\right\} \tag{2.4}$$

For $\tau = 0$, the covariance function reduces to the variance σ^2 which may be written as

$$C_{xx}(0) = \sigma^2 = E\left\{[x(t) - \mu]^2\right\} = \overline{[x(t) - \mu]^2} = \lim_{T\to\infty} \frac{1}{T} \int_0^T [x(t) - \mu]^2 \, dt \quad (2.5)$$

For a zero mean, the covariance function is identical to the autocorrelation function, i. e.,

$$R_{xx}(\tau) = C_{xx}(\tau) \quad \text{when} \quad \mu = 0 \quad (2.6)$$

The cross-covariance function $C_{xy}(\tau)$ is still another second order moment and is defined as

$$C_{xy}(\tau) = E\left\{[x(t) - \mu_x][y(t) + \tau) - \mu_y]\right\} \quad (2.7)$$

For zero mean values, Eq. (2.7) reduces to the cross-correlation function which appears as

$$R_{xy}(\tau) = E\left\{[x(t)][y(t+\tau)]\right\} \quad (2.8)$$

Consequently, for zero mean values, the cross-covariance function and the cross-correlation function are identities. $R_{xy}(0)$ has no particular significant statistical meaning.

The frequency composition of $x(t)$ may be described by the Fourier transform of the autocorrelation function which appears as

$$S_{xx}(f) = \int_{-\infty}^{\infty} R_{xx}(\tau)\, e^{-i2\pi f\tau} \, d\tau \quad (2.9)$$

where $S_{xx}(f)$ is shown in terms of cyclical frequencies and is called the power spectral density function with the units of mean square value per cps. As

defined here, $S_{xx}(f)$ is a two-sided function where f ranges from $-\infty$ to ∞, and is related to the spectral density in radians per second as $S_{xx}(f) = 2\pi S_{xx}(\omega)$. Since the autocorrelation function is symmetric with τ, then the imaginary part of Eq. (2.9) may be deleted so that

$$S_{xx}(f) = \int_{-\infty}^{\infty} R_{xx}(\tau) \cos 2\pi f\tau \, d\tau \tag{2.10}$$

The cross-spectrum may be written as

$$S_{xy}(f) = \int_{-\infty}^{\infty} R_{xy}(\tau) \, e^{-i2\pi f\tau} \, d\tau \tag{2.11}$$

The real part of the cross-spectrum is called the co-spectrum and the imaginary part of the cross-spectrum is called the quad-spectrum.

Given that $y(t)$ defines the output response of a linear time invariant mechanical system due to the input excitation $x(t)$, the relationship between the input and response power spectral densities is given by

$$S_{yy}(f) = |H(f)|^2 \, S_{xx}(f) \tag{2.12}$$

where $H(f)$ is the frequency response function for the linear system. Similarly, the cross-spectrum is related to the excitation power spectral density by

$$S_{xy}(f) = H(f) \, S_{xx}(f) \tag{2.13}$$

Other such relationships are given in Reference 3.

For distributed elastic structures, the preceding statistical definitions must be modified to account for spatial dependence as the response and excitation are both functions of space as well as time. Rather than dwell at this point on the statistical properties of distributed structures, the reader

is directed to Reference 4. For a practical interpretation of these statistical properties as applied to the testing of structures, the reader is directed to References 5 and 6.

2.2 NONSTATIONARY CONDITIONS

As contrasted to the statistical moments for ergodic random processes, the statistical moments for nonstationary processes are time dependent and are calculated by averaging over an ensemble of records instead of time averaging a single record. Time averaging, however, can be performed but the interpretation of these results is not obvious as is discussed in References 7 and 8.

Assuming that $x(t)$ is from a nonstationary random process, the mean is given as

$$\mu(t) = E[x(t)] \tag{2.14}$$

The autocorrelation function appears as

$$R_{xx}(t_1, t_2) = E[x(t_1)\, x(t_2)] \tag{2.15}$$

Letting $t_1 = t_2 = t$, the autocorrelation function reduces to the mean square value defined as

$$\psi^2(t) = E[x^2(t)] \tag{2.16}$$

The covariance function may be written as

$$C_{xx}(t_1, t_2) = E\left\{[x(t_1) - \mu(t_1)]\,[x(t_2) \quad \mu(t_2)]\right\} \tag{2.17}$$

Letting $t_1 = t_2 = t$, the covariance function reduces to the variance of $x(t)$ which may be written as

$$\sigma^2(t) = E\left\{[x(t) - \mu(t)]^2\right\} \tag{2.18}$$

For a zero mean value over all time, the covariance function becomes identical to the autocorrelation function; i.e., when $\mu(t) = 0$,

$$R_{xx}(t) = C_{xx}(t) \tag{2.19}$$

The cross-covariance function may be written as

$$C_{xy}(t_1, t_2) = E\left\{[x(t_1) - \mu_x(t_1)][y(t_2) - \mu_y(t_2)]\right\} \tag{2.20}$$

For zero mean values, the cross-covariance function reduces to the cross-correlation function $R_{xy}(t_1, t_2)$ which may be expressed as

$$R_{xy}(t_1, t_2) = E\left\{[x(t_1)][y(t_2)]\right\} \tag{2.21}$$

Basic relationships between the input and output power spectral density, the cross-spectral density, and the frequency response functions for a linear system are discussed in Section 5 of Reference 9.

3. RESPONSE OF A MECHANICAL OSCILLATOR

This section deals with approximate solutions to the two questions cited in the introduction regarding the oscillator response to stationary white noise and pulsed random excitation. It is recalled that the first question deals with the maximum response attained in time T with probability $P_M(\beta)$ whereas the second question considers the time duration for the oscillator to effectively attain stationarity in its response.

As one answer to the second question, Section 3.1 paraphrases the work of Caughey and Stumpf (Reference 10) where the excitation is white noise shaped by the unit step function. Section 3.2 considers an analog study by Barnoski and MacNeal (Reference 11) which provides an empirical solution to the first question when the excitation is stationary. Section 3.3 discusses analog data by Barnoski and MacNeal (Reference 12) which provide empirical solutions to both questions for nonstationary random excitation.

3.1 RESPONSE TO WHITE NOISE SHAPED IN TIME BY THE STEP FUNCTION

Much of the literature concerning the response of simple mechanical systems to stationary random excitation considers only the stationary aspects of the dynamic response. In including the transient motion of the mechanical oscillator, the response of the system to white noise shaped by the step function is nonstationary for the initial intervals of time. Two excellent papers in this subject area are found in References 10 and 13.

In keeping with the discussion of Reference 10, the equation of motion for the mechanical oscillator acted upon by a random acceleration excitation applied to the mass may be written as

$$\ddot{x} + 2\omega_n \zeta \dot{x} + \omega_n^2 x = \alpha(t) \qquad (3.1)$$

where

ζ = damping ratio of the mechanical oscillator

x = displacement of the mass from static equilibrium

$\dot{x}$ = velocity of the mass

$\ddot{x}$ = acceleration of the mass

ω_n = undamped natural frequency of the mechanical oscillator

$\alpha(t)$ = random acceleration acting on the mass

The undamped natural frequency and damping ratio are related to the physical parameters of the mechanical system by

$$\omega_n^2 = \frac{k}{m} \tag{3.2}$$

$$\zeta = \frac{c}{2m\omega_n} \tag{3.3}$$

where

k = linear spring constant

m = mass of the system

c = viscous damping coefficient

The random excitation is assumed to have the following properties

- $\alpha(t)$ is stationary
- $\alpha(t)$ is Gaussian
- $\alpha(t)$ has a zero mean value
- $\alpha(t)$ has the power spectrum $G_\alpha(\omega)$ which is considered to be smooth and contains no sharp peaks
- $\alpha(t)$ is assumed to be mean square continuous

Assuming small values of damping ($\zeta < 1$) and that the initial conditions are

$$x(0) = a; \quad \dot{x}(0) = b \tag{3.4}$$

then, a solution of (3.1) may be written as

$$x(t) = a\, e^{-\zeta \omega_n t}\left[\cos \omega_d t + \frac{\zeta \omega_n}{d} \sin \omega_d t\right]$$

$$+ \frac{b}{\omega_d}\, e^{-\zeta \omega_n t} \sin \omega_d t + \int_0^t h(t-\tau)\, \alpha(\tau)\, d\tau \tag{3.5}$$

where

$$\omega_d = \sqrt{1 - \zeta^2}\ \omega_n = \text{damped natural frequency of the oscillator} \tag{3.6}$$

and for $t \geq 0$

$$h(t) = \frac{e^{-\zeta \omega_n t}}{\omega_d} \sin \omega_d t = \text{impulse response of the system} \tag{3.7}$$

Since the response is noted to be a Gaussian process, only the mean and the variance need be calculated to characterize the response properties. The mean value of $x(t)$ is formed by an ensemble average and appears as

$$\mu(t) = E[x(t)] = a\, e^{-\omega_n \zeta t}\left[\cos \omega_d t + \frac{\omega_n t}{d} \sin \omega_d t\right]$$

$$+ \frac{b}{\omega_d}\, e^{-\omega_n \zeta t} \sin \omega_d t + \int_0^t h(t-\tau)\, E[\alpha(\tau)]\, d\tau \tag{3.8}$$

For the mean value of the excitation asumed equal to zero, the mean of the response appears as

$$\mu(t) = E[x(t)] = a\, e^{-\omega_n \zeta t}\left[\cos \omega_d t + \frac{\omega_n \zeta}{\omega_d} \sin \omega_d t\right]$$

$$+ \frac{b}{\omega_d} e^{-\omega_n \zeta t} \sin \omega_d t \qquad (3.9)$$

The variance of $x(t)$ is formed also by an ensemble average and is given as

$$\sigma^2(t) = E\left\{[x(t) - \mu(t)]^2\right\} \qquad (3.10)$$

In somewhat different form, the variance for the mechanical oscillator appears as

$$\sigma^2(t) = \int_0^t \int_0^t h(t - \tau)\, h(t - \tau')\, E[\alpha(\tau)\, \alpha(\tau')]\, d\tau\, d\tau' \qquad (3.11)$$

From Eq. (2.2), the expression containing the product of the acceleration terms is noted to be the autocorrelation function for $\alpha(\tau)$. This function may be written as

$$R_{\alpha\alpha}(\tau, \tau') = E[\alpha(\tau) \cdot \alpha(\tau')] \qquad (3.12)$$

Note that the τ nomenclature in Eq. (2.2) refers to a time difference whereas the τ symbols in Eq. (3.11) refer to variables of integration. For the stationary assumption, the autocorrelation function depends only on the time difference $(\tau - \tau')$ rather than on τ and τ' individually. Expressed in terms of the physically realizable one-sided power spectrum, Eq. (3.12) appears as

$$R_{\alpha\alpha}(\Delta t) = R_{\alpha\alpha}(\tau - \tau') = \int_0^\infty G_\alpha(\omega) \cos \omega(\tau - \tau')\, d\omega \qquad (3.13)$$

Substituting (3.13) and (3.7) into (3.11) and performing the double time integration yields

$$\sigma^2(t) = \int_0^\infty \frac{G_\alpha(\omega)}{|Z(\omega)|^2} \left\{ 1 + e^{-2\omega_n \zeta t} \left[1 + \frac{2\omega_n}{\omega_d} \zeta \sin \omega_d t \cos \omega_d t \right.\right.$$

$$- e^{\omega_n \zeta t} \left(2 \cos \omega_d t + \frac{2\omega_n \zeta}{\omega_d} \sin \omega_d t \right) \cos \omega t \qquad (3.14)$$

$$\left.\left. - e^{\omega_n \zeta t} \frac{2\omega}{\omega_d} \sin \omega_d t \sin \omega t + \frac{(\omega_n \zeta)^2 - \omega_d^2 + \omega^2}{\omega_d^2} \sin^2 \omega_d t \right] \right\} d\omega$$

where

$$|Z(\omega)|^2 = \left(\omega_n^2 - \omega^2\right)^2 + (2\omega\omega_n\zeta)^2 \qquad (3.15)$$

If $G_\alpha(\omega)$ is a smooth function of ω with no sharp peaks and $\zeta << 1$, then Eq. (3.14) can be approximated by Laplace's method of evaluating integrals which provides

$$\sigma^2(t) \simeq \frac{\pi G_\alpha(\omega_n)}{4\zeta\omega_n^3} \left\{ 1 - \frac{e^{-2\omega_n\zeta t}}{\omega_d^2} \left[\omega_d^2 + \frac{(2\omega_n\zeta)^2}{2} \sin^2 \omega_d t + \omega_n \omega_d \zeta \sin 2\omega_d t \right] \right\} \qquad (3.16)$$

where $G_\alpha(\omega_n)$ denotes the magnitude of $G_\alpha(\omega)$ at ω_n. Alternatively, Eq. (3.16) can be expressed as a nondimensional variance in the form

$$\frac{2\sigma^2(t)}{\pi} \frac{\omega_n^3}{G_\alpha(\omega_n)} \simeq \frac{1}{2\zeta} \left\{ 1 - e^{-2\zeta\omega_n t} \left[1 + \frac{2\zeta^2}{1-\zeta^2} \sin^2 \left(1-\zeta^2\right)^{\frac{1}{2}} \omega_n t \right.\right.$$

$$\left.\left. + \frac{\zeta}{\left(1-\zeta^2\right)^{\frac{1}{2}}} \sin 2 \left(1-\zeta^2\right)^{\frac{1}{2}} \omega_n t \right] \right\} \qquad (3.17)$$

Figure 2 is a family of curves of Eq. (3.17) for various values of damping ζ and is an extension of the same plot shown in Reference 10. All curves

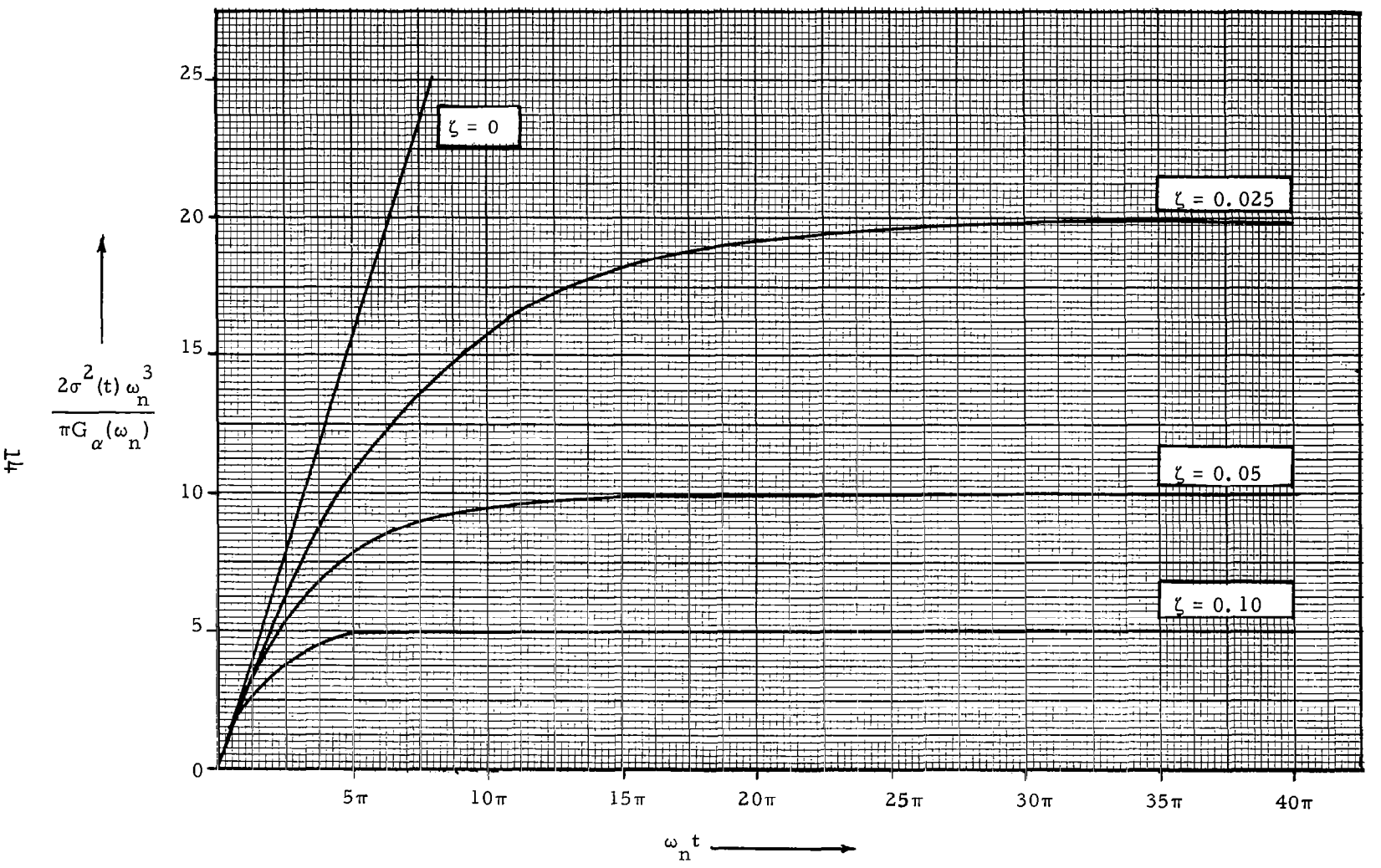

Figure 2. Dimensionless Variance of the Displacement Response of a Mechanical Oscillator Excited by White Noise Shaped in Time by the Step Function

begin at zero and, except for $\zeta = 0$, asymptotically approach $1/2\zeta$ as limiting values. Of particular interest is the value of $\omega_n t$ as the magnitude of the ordinate approaches an asymptotic value. This value yields the time or number of cycles for the mechanical oscillator to attain stationarity in its response. For example, $\omega_n t \sim 6\pi$ when $\zeta = 0.10$; this corresponds to approximately three cycles for the system response to achieve stationarity.

3.2 PEAK RESPONSE PROPERTIES TO STATIONARY RANDOM EXCITATION

The probability density is not yet known for the distribution in time of the peak response of a mechanical oscillator excited by white noise. Rice (page 223 of Reference 1), however, derived a probability density for the envelope maxima of the output from an ideal rectangular bandpass filter excited by white noise. In addition, Rice showed that the average number of envelope maxima is

$$\mu_n = 0.641B \tag{3.18}$$

where B is the noise bandwidth of the filter. Aspinwall (Reference 14), in turn, defined a mechanical equivalent to the electrical ideal bandpass filter and used these two results of Rice to obtain an approximate answer to the question regarding the probability of exceeding a stated amplitude within a finite time interval. For completeness of this discussion, it is appropriate to paraphrase the arguments of Aspinwall.

An equivalent ideal bandpass filter is obtained in the following manner. In Figure 3, the frequency response characteristics are shown for both a rectangular bandpass filter and a mechanical oscillator. The ordinate is noted as an absolute value of the frequency response function and the x-axis is the ratio of the excitation frequency to the undamped natural frequency of the oscillator. B is shown as the bandwidth for an ideal rectangular filter.

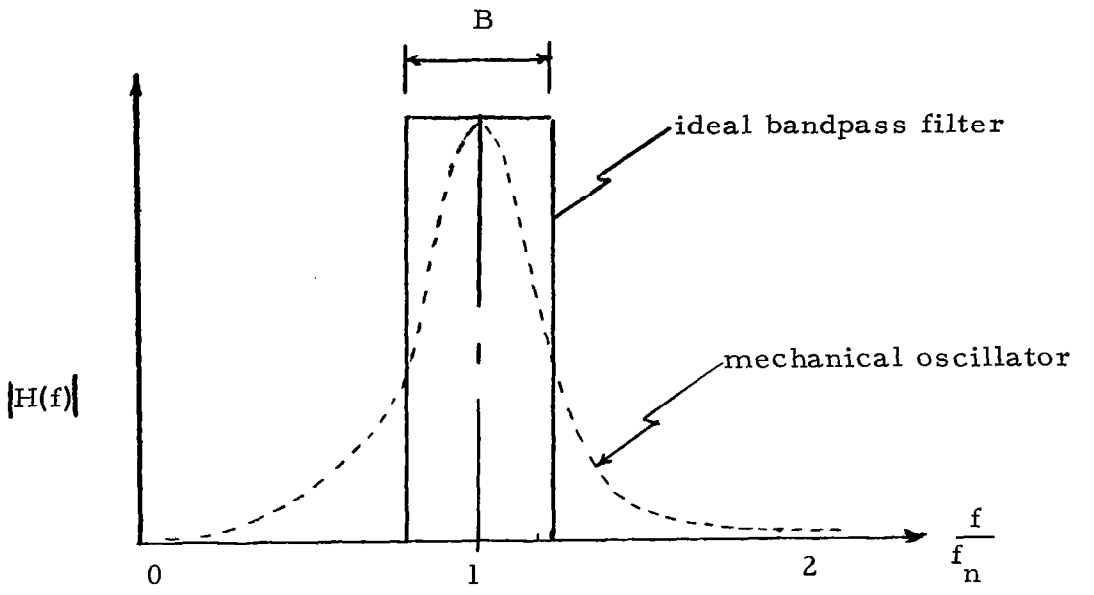

Figure 3. Magnitude of the Frequency Response Function for a Mechanical Oscillator and an Ideal Rectangular Bandpass Filter

The sketch for the mechanical oscillator depicts the magnitude of the velocity to force frequency response function for a mass excited oscillator. This function is expressed as

$$H(\omega) = \frac{\dot{x}}{f(t)} = \frac{1}{m}\left[\frac{1}{s + 2\zeta\omega_n + \frac{\omega_n^2}{s}}\right] = \frac{1/c}{1 + \frac{m}{c}s\left[1 + \frac{k}{ms^2}\right]} \qquad (3.19)$$

where $s = i\omega$ and other relationships are provided by Eqs. (3.2) and (3.3). In terms of the frequency in cycles per second, the absolute magnitude of (3.19) is

$$|H(f)| = \frac{2\pi f/k}{\sqrt{\left[2\zeta\frac{f}{f_n}\right]^2 + \left[1 - \left(\frac{f}{f_n}\right)^2\right]^2}} \qquad (3.20)$$

As shown by the sketch in Figure 3, Eq. (3.20) is zero at both extremes of the frequency axis and,for small values of damping, has a maximum value given approximately by

$$|H(f)|_{max} = \frac{\pi f_n}{\zeta k} = \frac{1}{c} \tag{3.21}$$

Bandwidth equivalence between the ideal bandpass filter and the mechanical oscillator is defined by requiring the output responses to white noise to have the same mean square value. It is tacitly assumed and shown in Figure 3 that the center frequencies and gain for both systems are the same. Thus, the mean square responses to white noise are

mechanical oscillator

$$\overline{\dot{x}^2} = \frac{\pi}{2} \frac{f_n}{Q} \cdot |H(f)|^2_{max} \cdot G_0(f) \tag{3.22}$$

ideal bandpass filter

$$\overline{\dot{x}^2} = B \cdot |H(f)|^2_{max} \cdot G_0(f) \tag{3.23}$$

where B is the noise bandwidth, $|H(f)|^2_{max}$ is the square of the maximum value of the frequency response function, and $G_0(f)$ is the magnitude of the white noise input excitation. Equating (3.22) and (3.23) yields the following relationship between the filter noise bandwidth and the oscillator half-power point bandwidth

$$B = \frac{\pi}{2} B_r \tag{3.24}$$

where the half-power point bandwidth is

$$B_r = \frac{f_n}{Q} \tag{3.25}$$

Substituting Eq. (3.24) into Eq. (3.18) yields the average number of envelope maxima as

$$\mu_n \simeq \frac{f_n}{Q} \tag{3.26}$$

Alternatively, substituting (3.21) into (3.22) yields the mean square velocity response as

$$\overline{\dot{x}^2} = \frac{Q}{4} G_0(f) \frac{\omega_n^3}{k^2} \tag{3.27}$$

Having an estimate for μ_n, an expression for predicting the probability of exceeding a given amplitude within a finite time interval is argued as follows. If it is assumed that the envelope maxima are independent random variables and that the number of envelope maxima for the time interval T is given by $\mu_n T$, THEN the occurrence of each envelope maxima is one of $\mu_n T$ Bernoulli trials where success is attained if the maxima $< \beta$. The probability that the maximum value of the envelope maxima remains $< \beta$ during the time interval T is then given as

$$P_M(\beta) = \left[P_E(\beta)\right]^{\mu_n T} \tag{3.28}$$

where

$P_M(\beta)$ is the probability that M, the maximum value for the envelope peaks in time T, is $\leq \beta$ times the rms value of the response

$P_E(\beta)$ is the probability that the maximum value of any envelope peak is $\leq \beta$ times the rms value of the output response. For the ideal bandpass filter, this value is obtained by integrating the probability density function of the envelope maxima (Reference 1, page 223) over the limits of interest.

$\mu_n T$ is the average number of envelope maxima during time T

μ_n is the average number of envelope maxima per second

T is the time interval for observing the output response

Alternatively, the probability of an envelope maxima exceeding β in time T is expressed as

$$P_M(>\beta) = 1 - P_M(\beta) \tag{3.29}$$

By way of interpreting Eqs. (3.28) and (3.29) consider their application to this classic statistical problem of flipping a single coin; what is the probability of flipping five heads in a row? For this problem, Eq. (3.28) can be used directly. In this context,

$P_M(\beta)$	denotes the probability of flipping five heads in a row
$P_E(\beta)$	denotes the probability of flipping a head in a single toss of the coin, that is 1/2
$\mu_n T$	denotes the total number of trials or flips of the coin, which, in this example, equals five

so that

$$P_M(\beta) = (1/2)^5 = 0.031 \tag{3.30}$$

From Eq. (3.29), the probability of not flipping five heads in a row is simply

$$P_M(>\beta) = 1 - .031 = 0.969 \tag{3.31}$$

Substituting (3.26) into (3.28) yields $P_M(\beta)$ for the mechanical oscillator as

$$P_M(\beta) = \left[P_E(\beta)\right]^{T^*} \tag{3.32}$$

where

$$T^* = \frac{f_n T}{Q} \tag{3.33}$$

T^* is noted as a dimensionless time parameter and $f_n T$ may be interpreted as the number of cycles for which the random response is observed. The $P_E(\beta)$ term is obtained directly from the probability density for envelope maxima given by Rice on page 223 of Reference 1.

As sketched in Figure 4, Eq. (3.32) can be displayed as a family of probability curves in $P_M(\beta)$ plotted as log T^* versus β. These curves represent the results of a theoretical development by Aspinwall and are appropriately called Aspinwall curves in this report. It is remembered that these curves are applicable to the peak properties of the stationary response for a lightly damped mechanical oscillator where the excitation is stationary white noise.

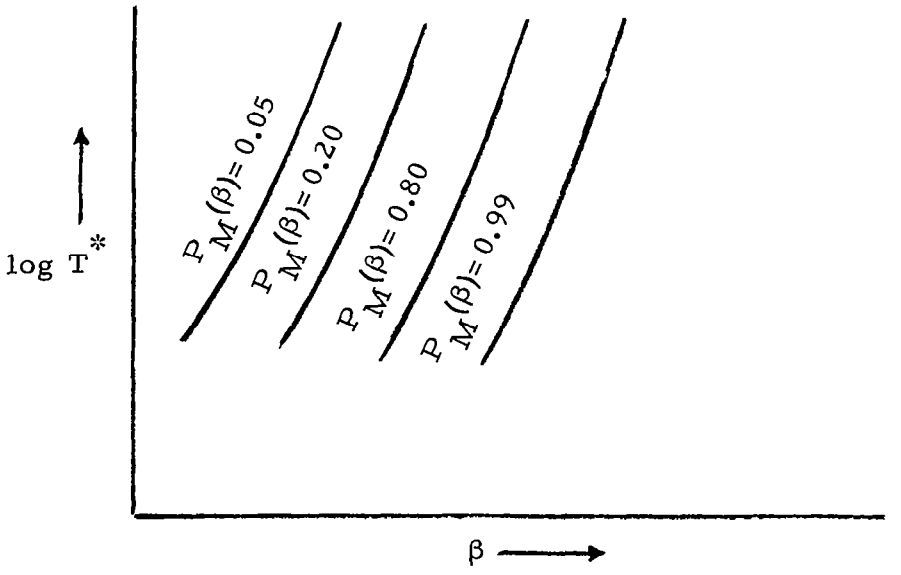

Figure 4. Parametric Plot for the Peak to RMS Response of a Mechanical Oscillator Subjected to Broadband Stationary Random Excitation

As mentioned in Reference 14, the errors inherent in the Aspinwall curves are associated with the following assumptions:

(1) Differences between the actual number of envelope maxima and the approximate number given as $\mu_n T$.

(2) Differences in μ_n for the rectangular bandpass filter and the mechanical oscillator.

(3) Errors in assuming the $P_E(\beta)$ developed by Rice for an ideal rectangular filter to be directly applicable for the band-pass of the mechanical oscillator.

(4) Errors in assuming the envelope maxima to be statistically independent.

Although these factors bias the numerical results of the theoretical analysis, the trends displayed by the curves in Figure 4 were believed to be valid.

In Reference 11, Barnoski and MacNeal examined the validity of Aspinwall curves bycomparing these theoretical results with empirical data from an analog computer study. For this study, a mechanical oscillator was simulated by the operational amplifier circuits shown as Figure 5. The triangles denote simple electronic amplifiers, the K's represent potentiometers, C's are capacitors, R's are resistors, E_i is the input excitation and e represents the velocity of the mechanical system. In terms of the s operator, the ratio of the velocity to the input excitation is

$$\frac{e}{E_i} = \frac{\dfrac{K_3 R_3}{K_2 R_4}}{1 + \dfrac{R_3 C_1 s}{K_2}\left[1 + \dfrac{AK_1}{R_1 C_1 R_2 C_2 s^2}\right]}$$

Comparing the terms of (3.19) with (3.34) yields

$$\frac{1}{c} = \frac{K_3 R_3}{K_2 R_4} \tag{3.35}$$

$$\frac{Q}{\omega_n} = \frac{R_3 C_1}{K_2} \tag{3.36}$$

$$\omega_n^2 = \frac{AK_1}{R_1 C_1 R_2 C_2} \tag{3.37}$$

Selecting the appropriate values for the components in (3.35), (3.36), and (3.37) guarantees the simulation of the velocity to force frequency response function for the mechanical oscillator.

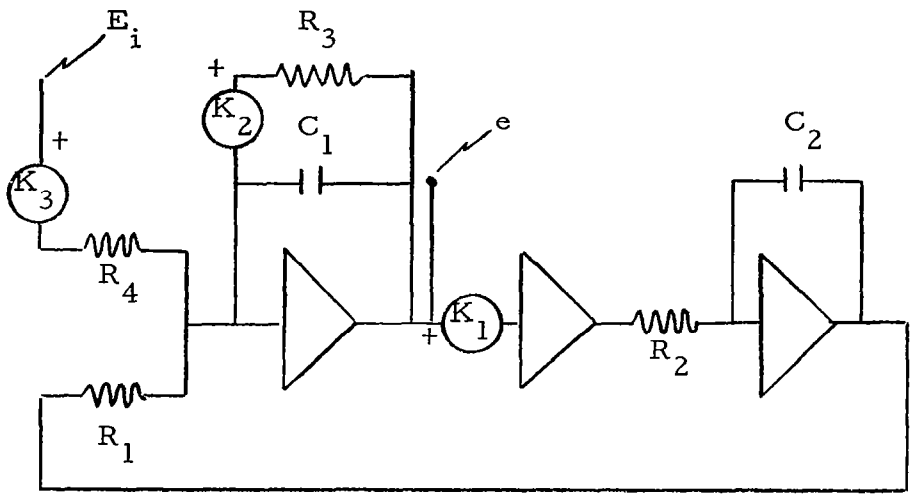

Figure 5. Operational Amplifier Circuits for a Linear Mechanical Oscillator

In the analog study, the oscillator was excited continuously by white noise and the velocity response was observed for time intervals (T) ranging from a minimum of 0.1 second to a maximum of 20 seconds. The white noise was provided by a random noise generator and the noise level was set so $\sim 6\sigma$ peaks of the output voltage would not be clipped by the amplifiers. For each time interval and value of f_n/Q, the output signal was sampled 100 times where the time duration for each sampling was T seconds. Figure 6 shows two typical time histories as observed during the sampling interval $T = 0.1$ second, and where $Q = 20$ and $f_n = 318$ cps.

For each sampling, the maximum positive and negative values for the output signal was measured and recorded. After 100 samplings, these data then were arranged in rank order to yield histograms of probability versus β.

Through each histogram, a mean curve was drawn which represents an empirical plot of $P_M(\beta)$ versus β. These empirical curves were used to create empirical plots of $f_n T/Q$ versus β for values of $P_M(\beta)$ as illustrated by Figures 7 and 8.

The coordinates in these figures are noted to be the coordinates of Figure 4 so that the Aspinwall probability curves can be compared directly with the empirical curves. The empirical curves are plotted as a family in Q for Q values of 5, 10, 20, and 50. Each data point shown was obtained from mean curves of the histograms alluded to in the previous paragraph. Also shown are the approximate number of cycles for which the oscillator was observed. It is interesting to note that for the larger values of $f_n T/Q$, the constant probability curves tend to appear as straight lines on the semi-log graph paper. This implies the $f_n T/Q$ and β are related in form as

$$\log \frac{f_n T}{Q} = m\beta + \text{constant} \tag{3.38}$$

where m is the slope of the straight lines.

From Figures 7 and 8, it can be concluded that the empirical data lend support to the theory embodied in Aspinwall curves although the response ratios (β) are consistently higher than those predicted by the Aspinwall theory. In other words, the numerical values provided by the theoretical curves are not conservative. By noting the vertical alignment of data points for the larger number of cycles, it may be concluded that the response ratio (β) tends to become independent of Q for a large number of cycles.

Figure 9 is a family of curves in $P_M(\beta)$ for the peak to rms response ratio (β) versus the dimensionless time parameter ($f_n T/Q$). These curves are based on the empirical plots from Figures 7 and 8, as well as similar data from Reference 12. Only two values of $P_M(\beta)$ are shown and each $P_M(\beta)$ curve is noted to be influenced by the damping values of the oscillator.

The β ordinate values where $T = 0$ become the instantaneous values of the amplitude time history. Since the probability density of the instantaneous values is normal, these magnitudes are obtained from most any tabulated table of the Gaussian density function. All the curves of Figure 9 exhibit a rapid rise in the β value for initial intervals of $f_n T/Q$. After passing through a knee in the vicinity of $f_n T/Q = 1$, the β values increase very slowly for relatively large increases in $f_n T/Q$. Although the plots are shown only up to $f_n T/Q = 7$, it is understood that these curves, in the limit, extend to infinity where the β ratio theoretically becomes infinite. Thus, an infinite peak is to be expected in an infinite time.

The curves of Figure 9 show that peak to rms response ratios of $3[P_M(\beta) = 0.60]$ and $4[P_M(\beta) = 0.95]$ are not uncommon in short time intervals for a linear oscillator. On the other hand, a large time lapse is required before β ratios of 5 or 6 are expected. These curves assume significance to a designer if they are applied to establish structural reliability criteria based on a time dependent probability of extreme loads. In addition, these curves can be used to define stationarity in the peak response as the shown plots are the stationary results of an oscillator excited by stationary white noise.

Figure 10 depicts families of curves in $P_M(\beta)$ for the peak to rms response ratio plotted versus the number of cycles for the oscillator ($f_n T$). The equation for this theoretical boundary was developed by Thrall using non-parametric statistics (Reference 15) and can be expressed as

$$f_n T = \frac{[1 - P_M(\beta)]}{2} e^{\beta^2/2} \tag{3.39}$$

The shown theoretical curve is only for $P_M(\beta) = 0.95$ whereas the remaining $P_M(\beta)$ plots are empirical plots formed from the analog data of Figures 7 and 8. Figure 10 clearly points out that the β response ratio becomes independent

of the oscillator damping for a large number of cycles. Although the theoretical $P_M(\beta)$ plot is based upon an average value for the number of level crossings per unit time, Eq. (3.39) appears as a valid bound for large values of T. For small T values, however, the theoretical bound is noted to be inexact, but conservative, when compared with the empirical curves.

By comparing the Q curves for any value of $P_M(\beta)$, it is noticed in Figure 10 that the β values are higher for the larger damping values. This behavior requires further explanation. The output maxima response of an oscillator excited by white noise may be considered to consist of clumps of envelope maxima per unit time. For a very high Q system, the envelope maxima (clumps) are noted to be well separated in time. As damping is increased, the time separation between envelope maxima becomes less so that a greater number of maxima occur per unit time. Hence, the greater the clump density in time, the greater the likelihood of experiencing higher peak to rms values.

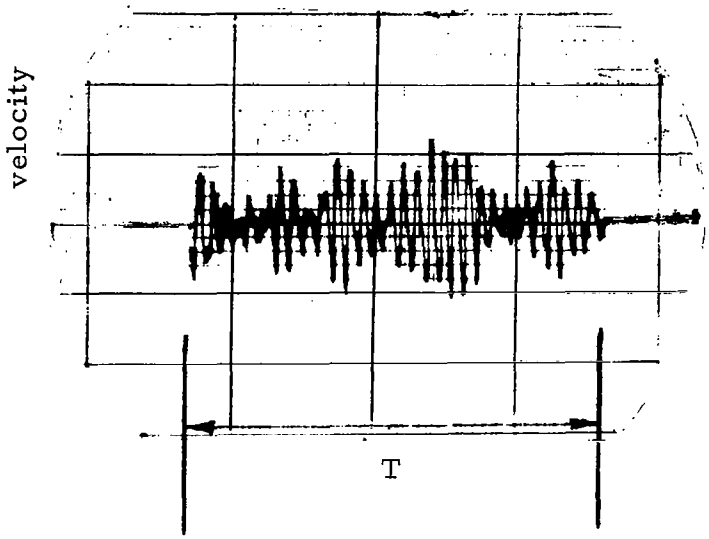

Typical Responses - Single Degree-of-Freedom System	
Stationary Conditions	
Q = 20	f_n = 318 cps
T = .1 sec.	T^* = 1.59

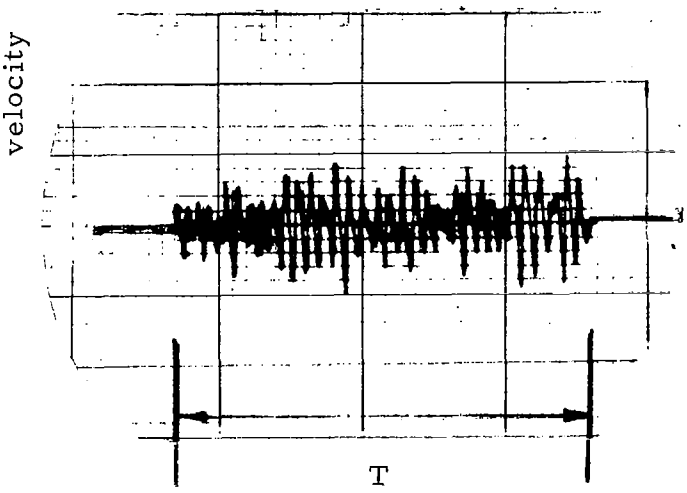

Figure 6. Two Typical Time Histories for the Response of a Mechanical Oscillator Excited by Stationary White Noise

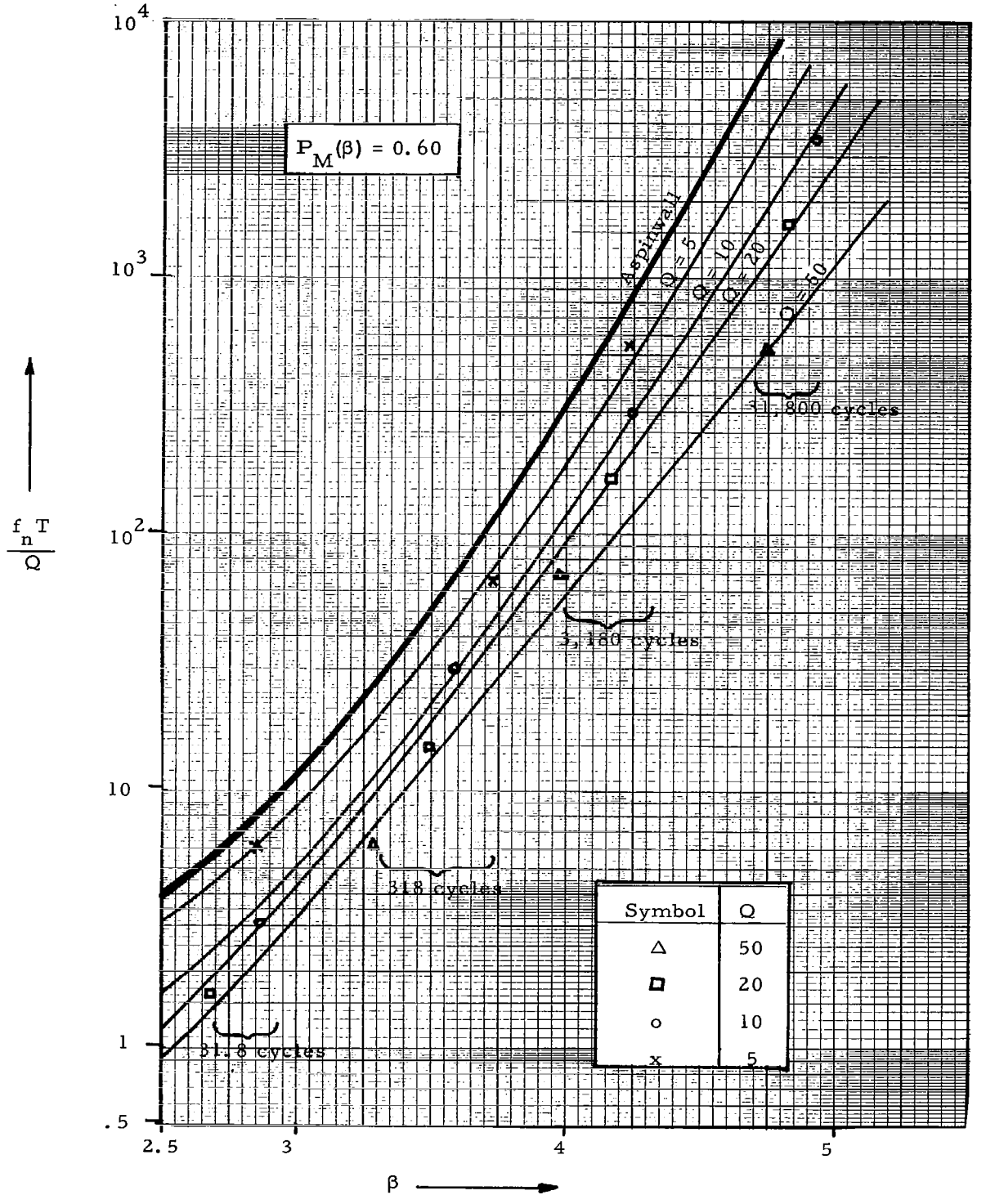

Figure 7. Dimensionless Time Parameter Versus the Ratio of Peak to RMS Response for the Output of a Mechanical Oscillator Excited by Stationary White Noise: $P_M(\beta) = 0.60$

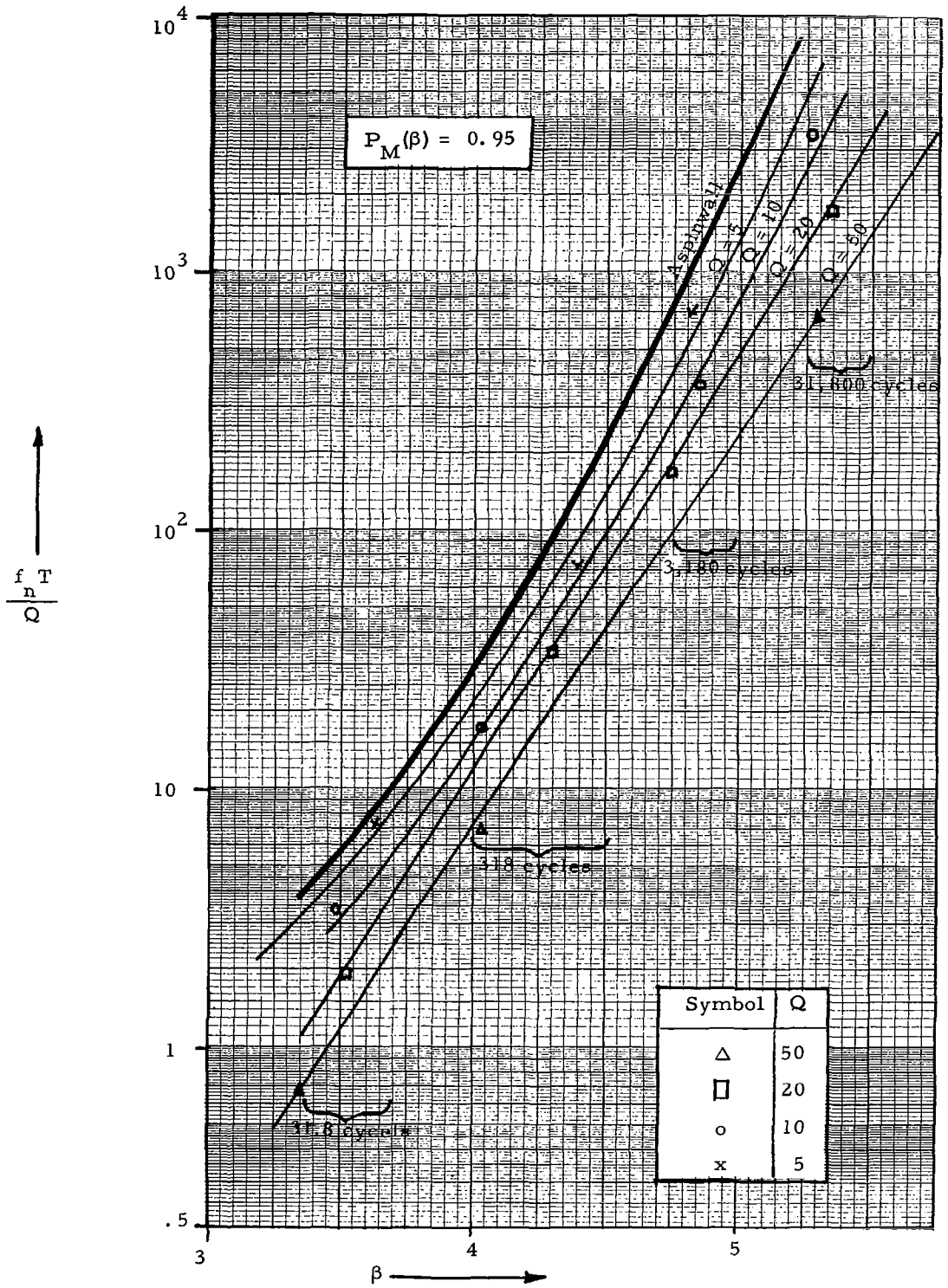

Figure 8. Dimensionless Time Parameter Versus Ratio of Peak to RMS Response for the Output of a Mechanical Oscillator Excited by Stationary White Noise: $P_M(\beta) = 0.95$

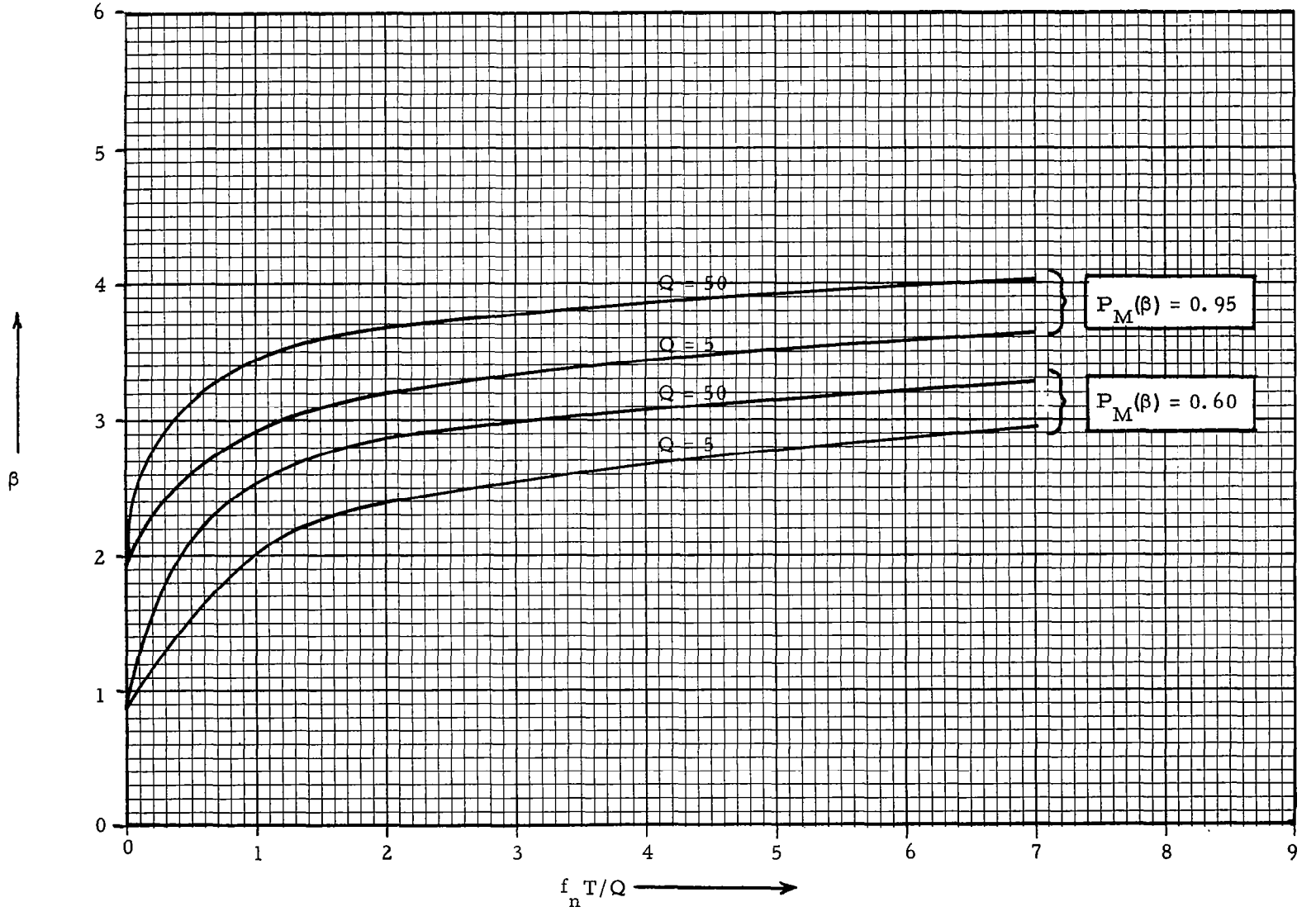

Figure 9. Experimental Envelope for the Peak to RMS Response of the Mechanical Oscillator Excited by Stationary White Noise (β versus $f_n T/Q$)

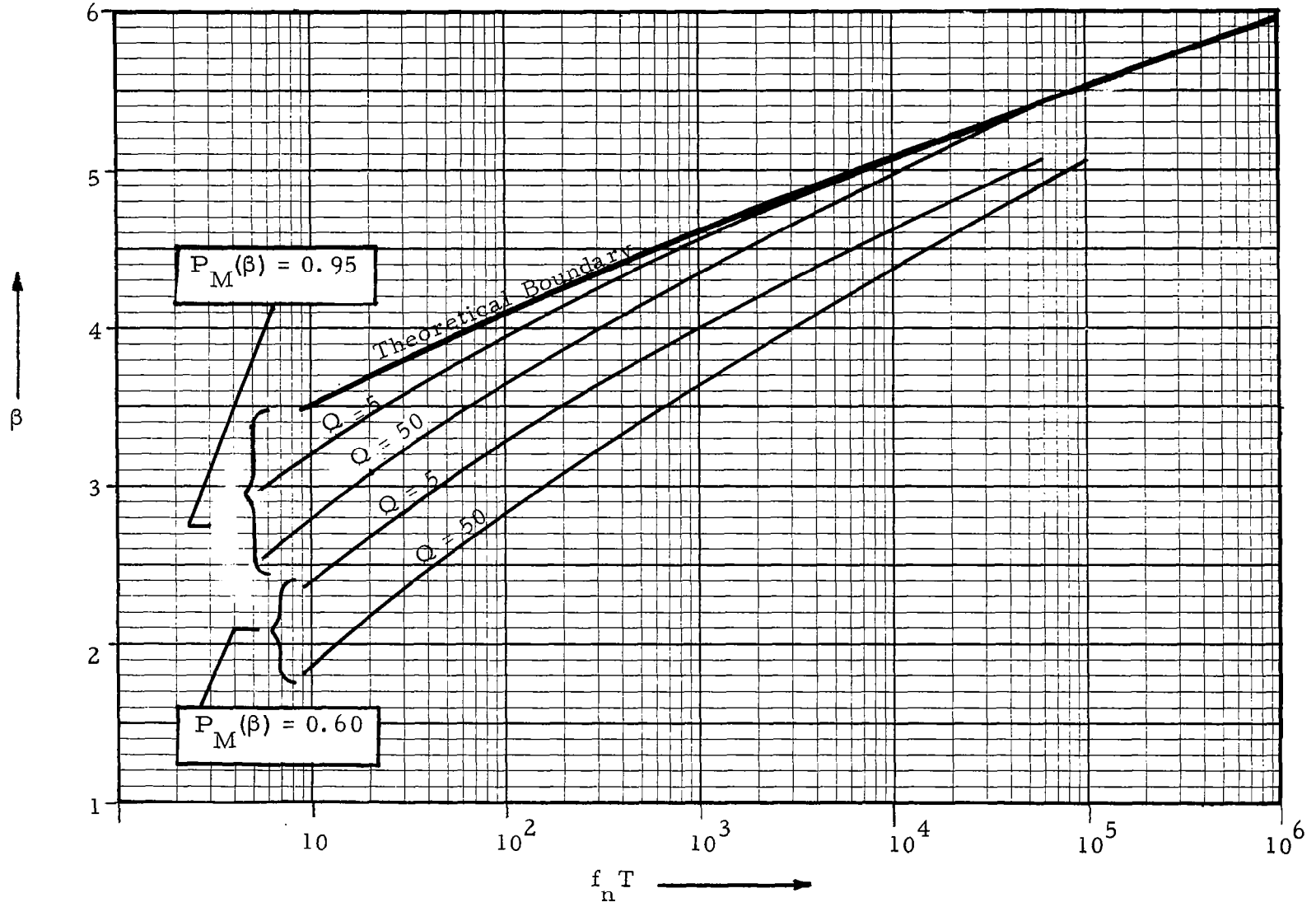

Figure 10. Experimental Results for the Peak to RMS Response of the Mechanical Oscillator Excited by Stationary White Noise (β versus $f_n T$)

3.3 PEAK RESPONSE PROPERTIES TO NONSTATIONARY RANDOM EXCITATION

Attention is focused in this section upon the peak response behavior of a mechanical oscillator when the excitation is white noise shaped in time by either a rectangular or half-sine envelope function. Hence, the excitation is nonstationary and appears as a pulse of white noise shaped either as a rectangle or a half-sine. This problem is typically associated with structural response to shock loading where the shock can be due to phenomenon as earthquakes, nuclear blasts, or missile launch. Barnoski and MacNeal (Reference 12) treated this problem for a linear oscillator using an analog computer and much of their data form the basis of this discussion.

To display the peak response results to nonstationary excitation using the $f_n T/Q$ and β parameters of the previous section, a time duration analogous to the sampling interval T need be defined. It is recalled that T refers to the time interval for sampling the response of the linear oscillator to stationary white noise. For the nonstationary study, the response is continuously monitored so that a time interval analogous to T is stated in terms of the duration of the input pulse. An effective or analogous time interval $\Delta\tau$ is defined by requiring the input energy in the nonstationary pulse to be equal to an equivalent amount of energy for stationary conditions. Hence, the nonstationary time interval is expressed as

$$\Delta\tau = \frac{1}{E_{max}^2} \int_0^\infty E^2(t)\, dt \tag{3.40}$$

where $E(t)$ is an envelope function denoted as

$$E(t) = E_{max}\, g(t) \tag{3.41}$$

E_{max} is the maximum value of the envelope function and g(t) is the shape function. For the rectangular and half-sine shape function, E(t) and the effective time intervals ($\Delta\tau$) for these pulses appear as shown in Figure 11.

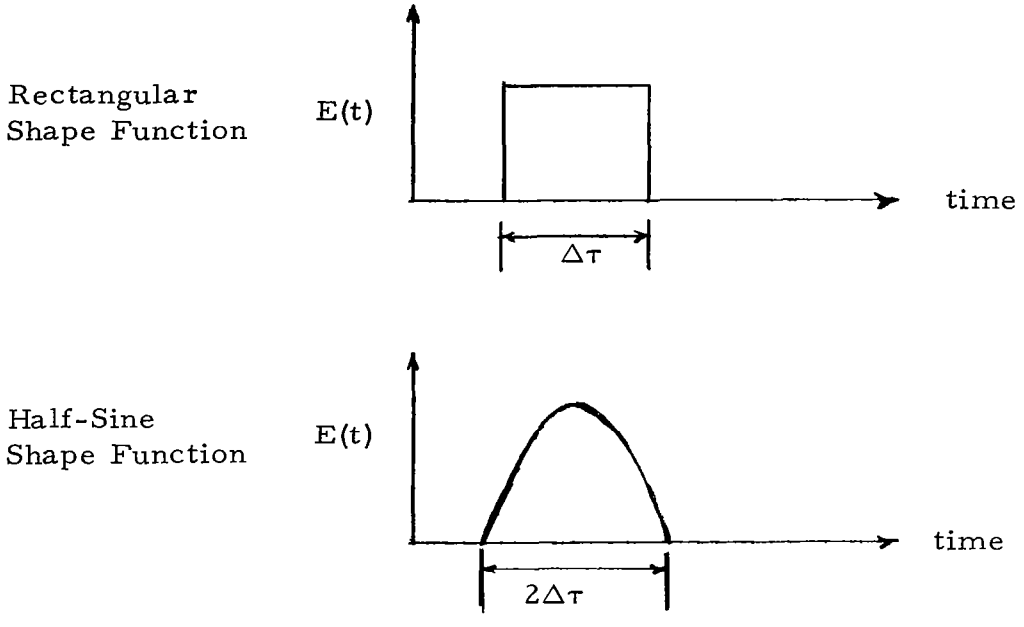

Figure 11. Rectangular and Half-Sine Envelope Functions for the Pulsed Random Excitation

Thus, the effective time interval for the rectangular pulse is equal to its actual time duration whereas the effective time interval for the half-sine pulse is one-half its actual time duration. It is to be noted that the rectangular shape function approaches a step function as $\Delta\tau$ becomes very large.

The dimensionless time parameter for the nonstationary conditions becomes

$$T^* = \frac{f_n \Delta\tau}{Q} \tag{3.42}$$

where Eq. (3.42) differs from Eq. (3.33) only in the definition of the time intervals T and $\Delta\tau$.

The expression for the pulsed excitation can be written as

$$f(t) = G_0 E(t) \tag{3.43}$$

where G_0 is the magnitude of the white noise spectrum. Equation (3.43) is created electrically by multiplying the outputs from a random noise source and an envelope generator.

In their analog study, Barnoski and MacNeal varied T^* in discrete steps ranging from a minimum value of 0.25 to a maximum value of 5.00. This maximum value of T^* is considered large enough so that $\Delta\tau$ is long compared to the natural period of the oscillator. For this condition, the input excitation appears as stationary white noise to the oscillator and the β response should be nearly the same as in Figure 9. The undamped natural frequency of the system (f_n) was set at 159 cps and Q values were 5, 20, and 50.

For a specified T^*, the oscillator was excited by either a rectangular pulse or a half-sine pulse of white noise and the maximum positive and negative values of the peak to rms time histories were recorded. This procedure was repeated 100 times for each T^* value. As with the analog data of Section 3.2, these recorded data were arranged in rank order to construct $P_M(\beta)$ versus β curves; then, to create the desired $f_n\Delta\tau/Q$ versus β plots.

Figure 12 shows a typical rectangular pulse of white noise and the resulting response of a linear oscillator to such an excitation. The experimental constants are $Q = 20$ and $\Delta\tau = 0.0314$ second which defines $T^* = f_n\Delta\tau/Q = 0.25$. The effective time interval ($\Delta\tau$) defined by Eq. (3.40) is equal to the actual time duration of the pulse and is noted to be five times the natural period of the oscillator. The response is a velocity time history and is observed as a damped harmonic oscillation after the pulse is terminated.

Figure 13 shows a half-sine envelope function and a typical resulting pulsed random excitation when this envelope function is multiplied with the

output of a random noise generator. This half-sine pulse of white noise has an effective time interval ($\Delta\tau$) of one-half the time duration of the envelope function. As with the rectangular pulse, the effective time duration is five times the period of the mechanical oscillator. Figure 14 depicts two typical responses of the oscillator when disturbed by the half-sine pulse of white noise. Such responses were continuously monitored and the positive and negative peak to rms values were recorded and used to form $P_M(\beta)$ versus β plots in a manner identical to that for the rectangular pulse.

The results of the analog study are summarized in Figures 15 through 20. These figures are families of curves in $P_M(\beta)$ for both stationary and nonstationary conditions with the peak to rms response ratio (β) plotted versus the dimensionless time parameter (T^*). Figures 15, 16, and 17 are the results for Q = 5, 20,and 50 respectively, when the nonstationary excitation is the rectangular pulse of white noise. Figures 18, 19, and 20 are the results for Q = 5, 20, and 50 respectively, when the nonstationary excitation is the half-sine pulse of white noise.

All of the curves exhibit the same characteristic behavior: that is a very rapid rise in β for the initial intervals of T^*, passing through a knee in the vicinity of $T^* = 1$, then increasing in β very slowly beyond the knee. As would be expected, the magnitudes of the curves for the pulsed nonstationary excitation are bounded by the stationary curves from Section 3.2. These figures, therefore, can be used to assess the time duration for an oscillator to effectively achieve stationarity in its response. Beyond $T^* = 1$, the β results for stationary white noise can be used for predicting peak to rms response values and are noted to yield conservative estimates for β in all cases.

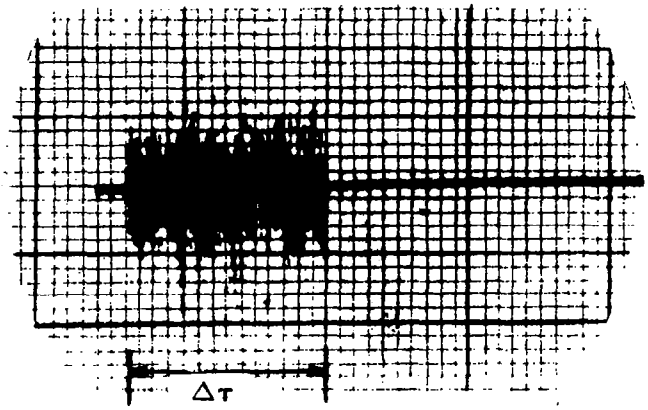

Pulsed Random Excitation
(Rectangular Envelope)

Mechanical Oscillator Nonstationary Problem	
Q = 20	f_n = 159 cps
Δτ = .0314 sec.	T^* = .25

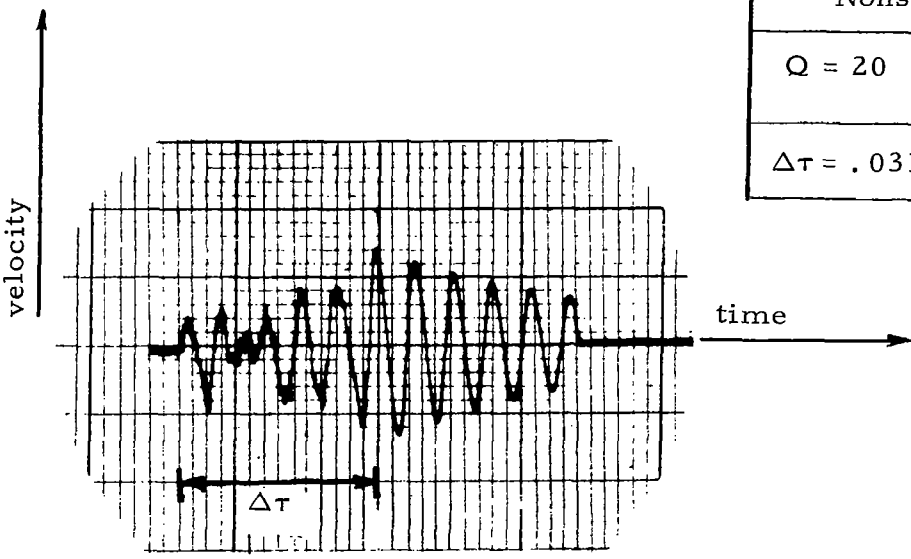

Typical Response

Figure 12. Typical Excitation and Response of the Mechanical Oscillator Subjected to Pulsed Random Excitation; Rectangular Envelope

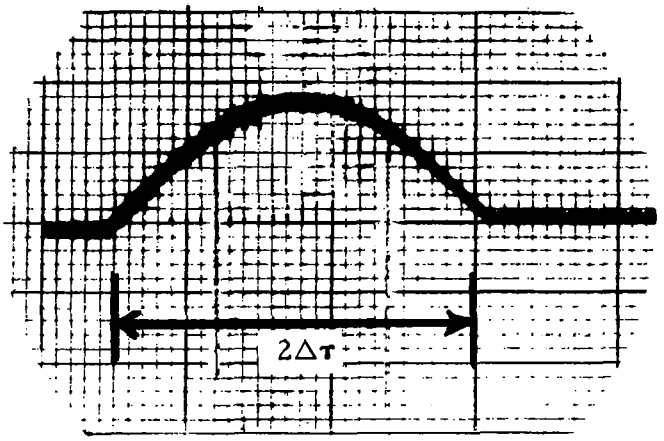

Half-Sine Envelope Function

Mechanical Oscillator Nonstationary Problem	
Q = 20	f_n = 159 cps
Δτ = .0314 sec.	T^* = .25

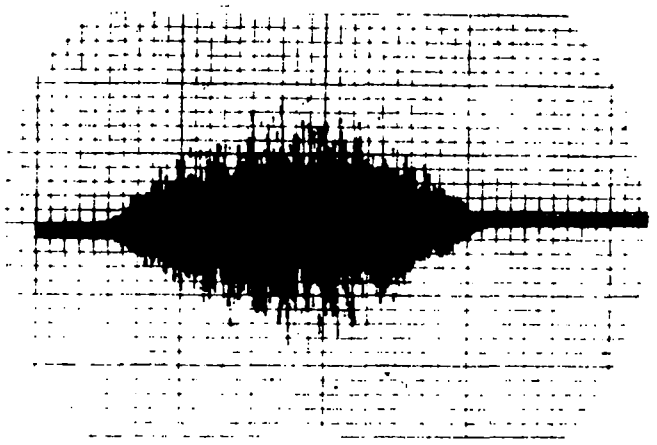

Pulsed Random Excitation

Figure 13. Typical Excitation of the Mechanical Oscillator Subjected to Pulsed Random Excitation; Half-Sine Envelope

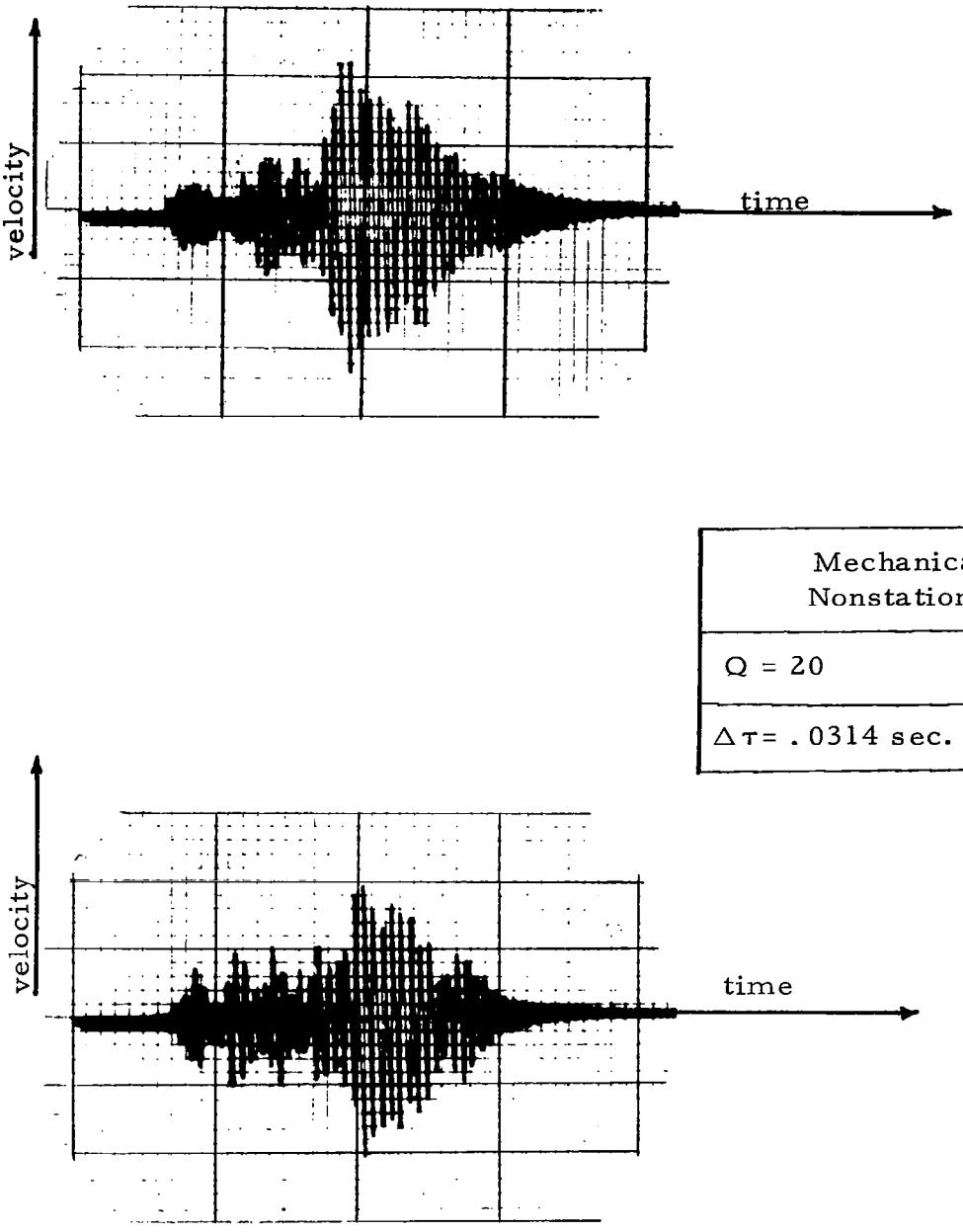

Figure 14. Typical Responses of the Mechanical Oscillator Subjected to Pulsed Random Excitation; Half-Sine Envelope

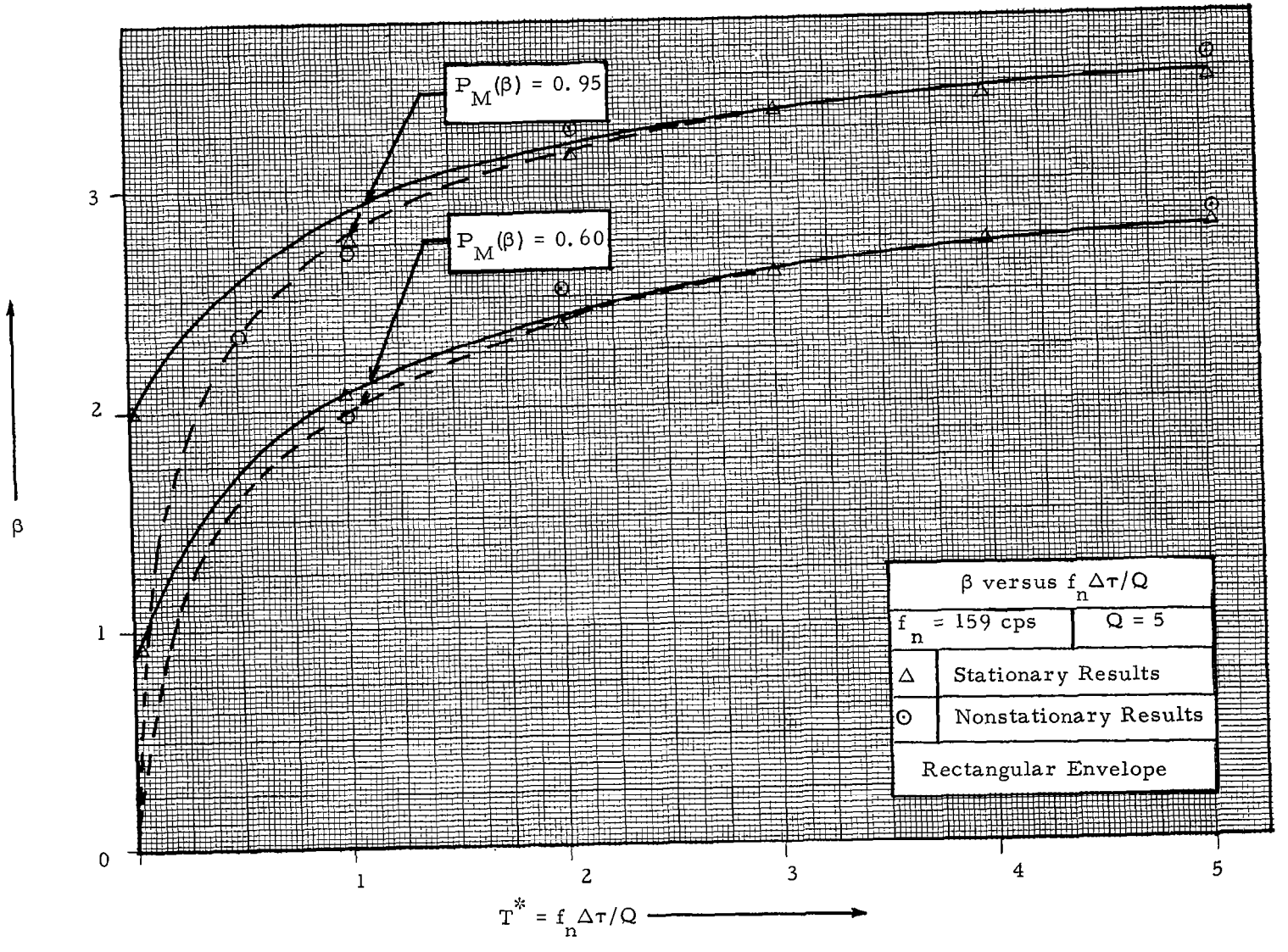

Figure 15. Ratio of Peak Response to RMS Response of the Mechanical Oscillator (β) Versus the Dimensionless Time Parameter (T^*) for Stationary and Pulsed Random Excitation. Rectangular Envelope, Q = 5

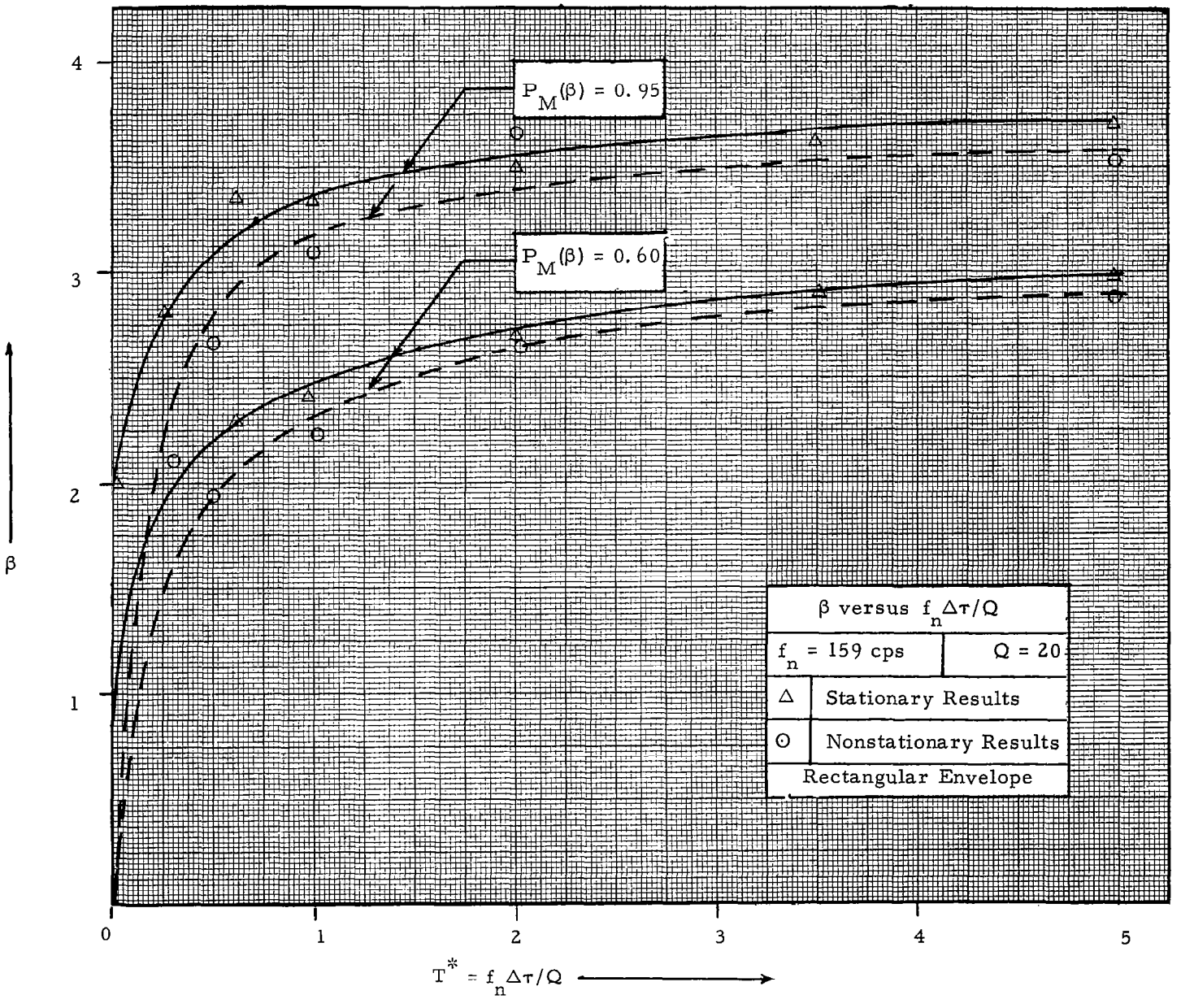

Figure 16. Ratio of Peak Response to RMS Response of the Mechanical Oscillator (β) versus the Dimensionless Time Parameter (T^*) for Stationary and Pulsed Random Excitation. Rectangular Envelope, Q = 20

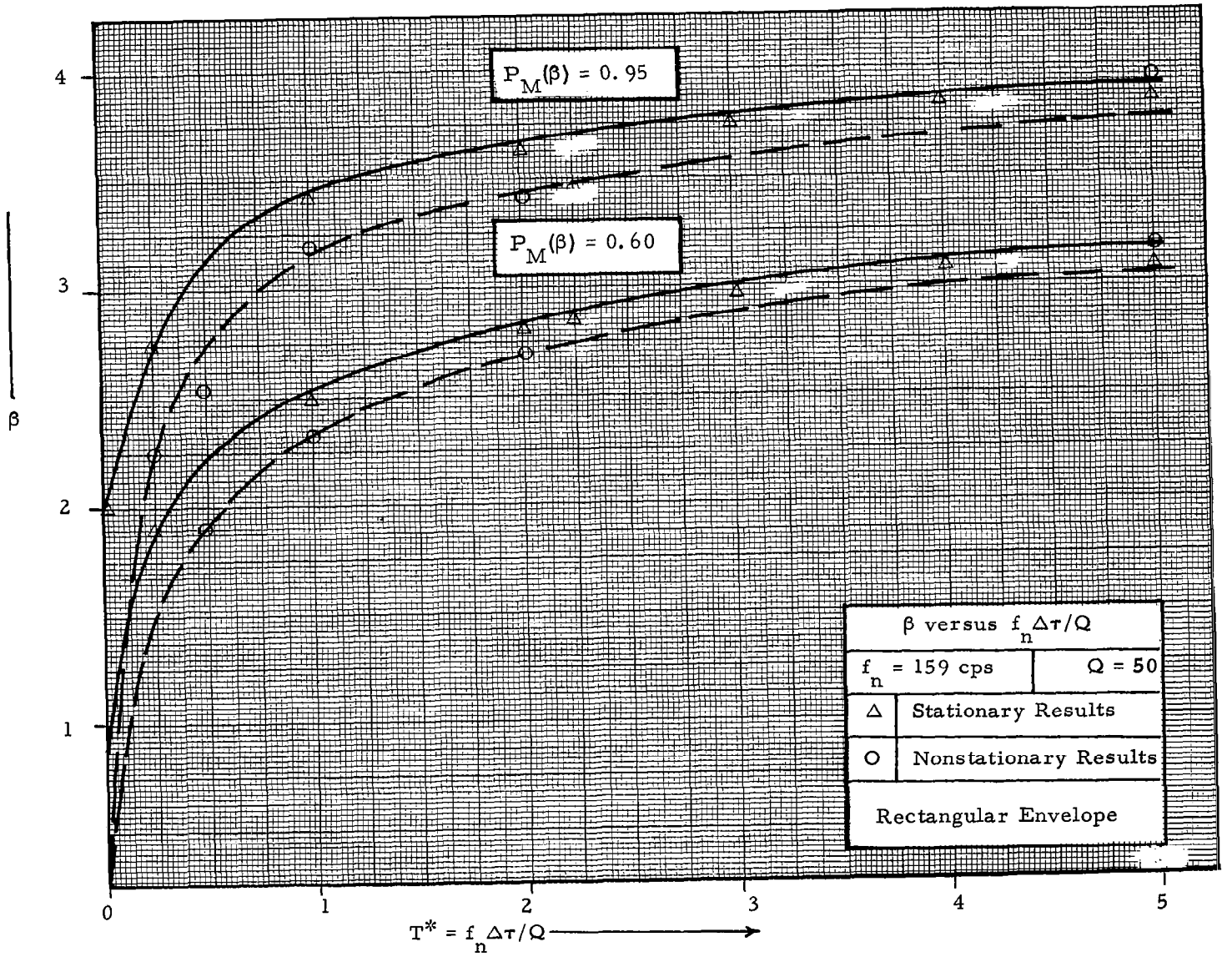

Figure 17. Ratio of Peak Response to RMS Response of the Mechanical Oscillator (β) versus the Dimensionless Time Parameter (T*) for Stationary and Pulsed Random Excitation. Rectangular Envelope, Q = 50

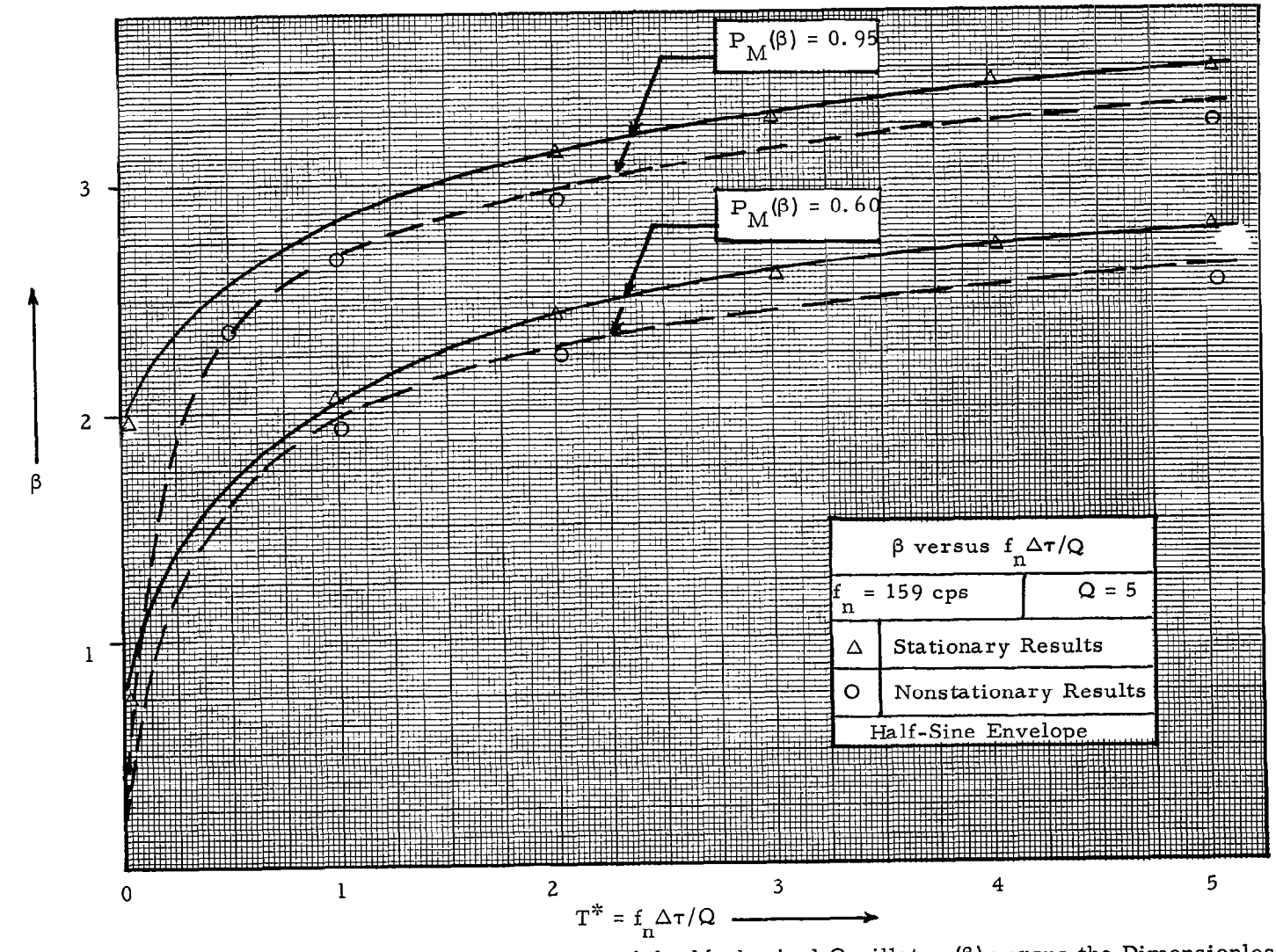

Figure 18. Ratio of Peak Response to RMS Response of the Mechanical Oscillator (β) versus the Dimensionless Time Parameter (T*) for Stationary and Pulsed Random Excitation. Half-Sine Envelope, Q = 5

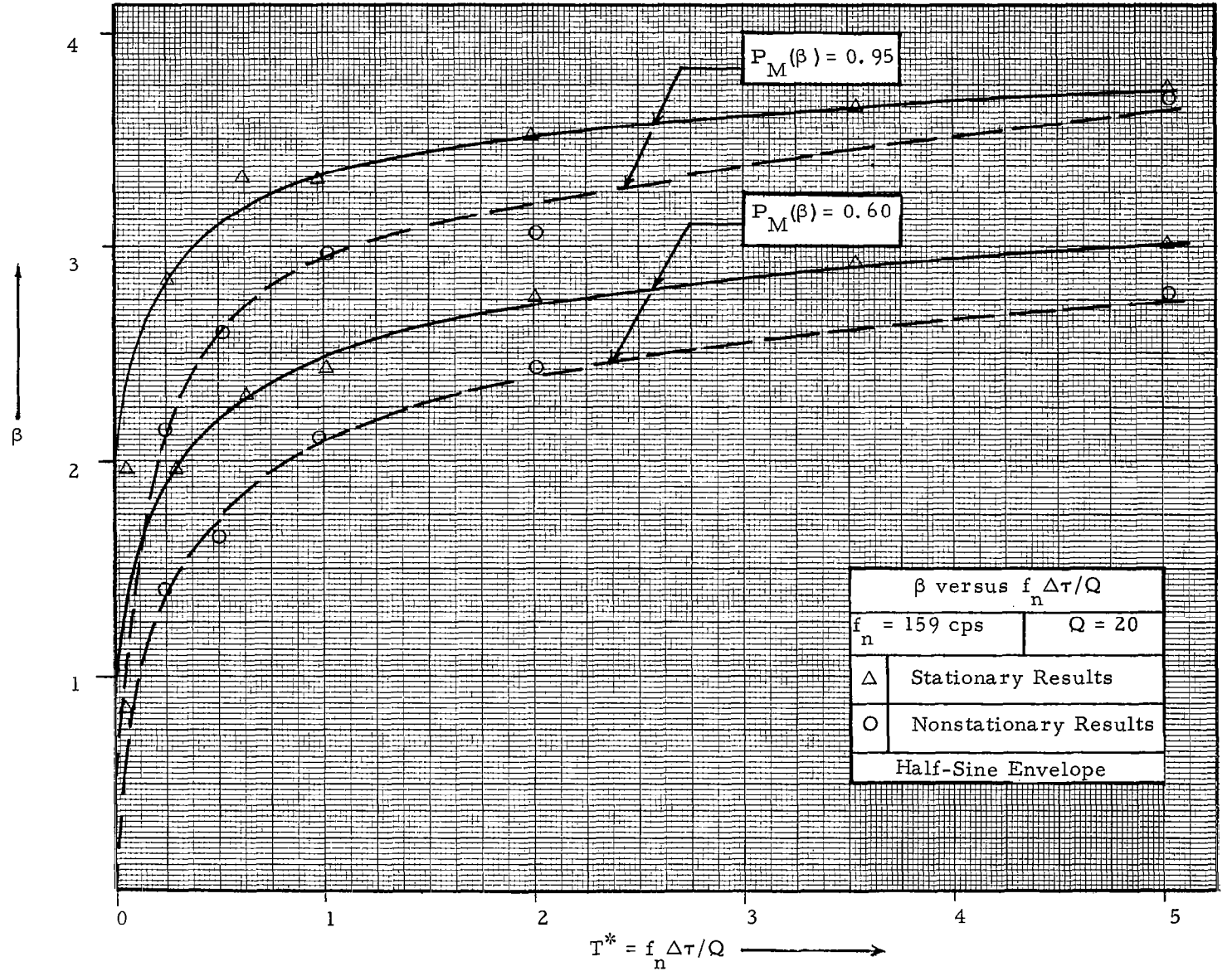

Figure 19. Ratio of Peak Response to RMS Response of the Mechanical Oscillator (β) versus the Dimensionless Time Parameter (T*) for Stationary and Pulsed Random Excitation. Half-Sine Envelope, Q = 20

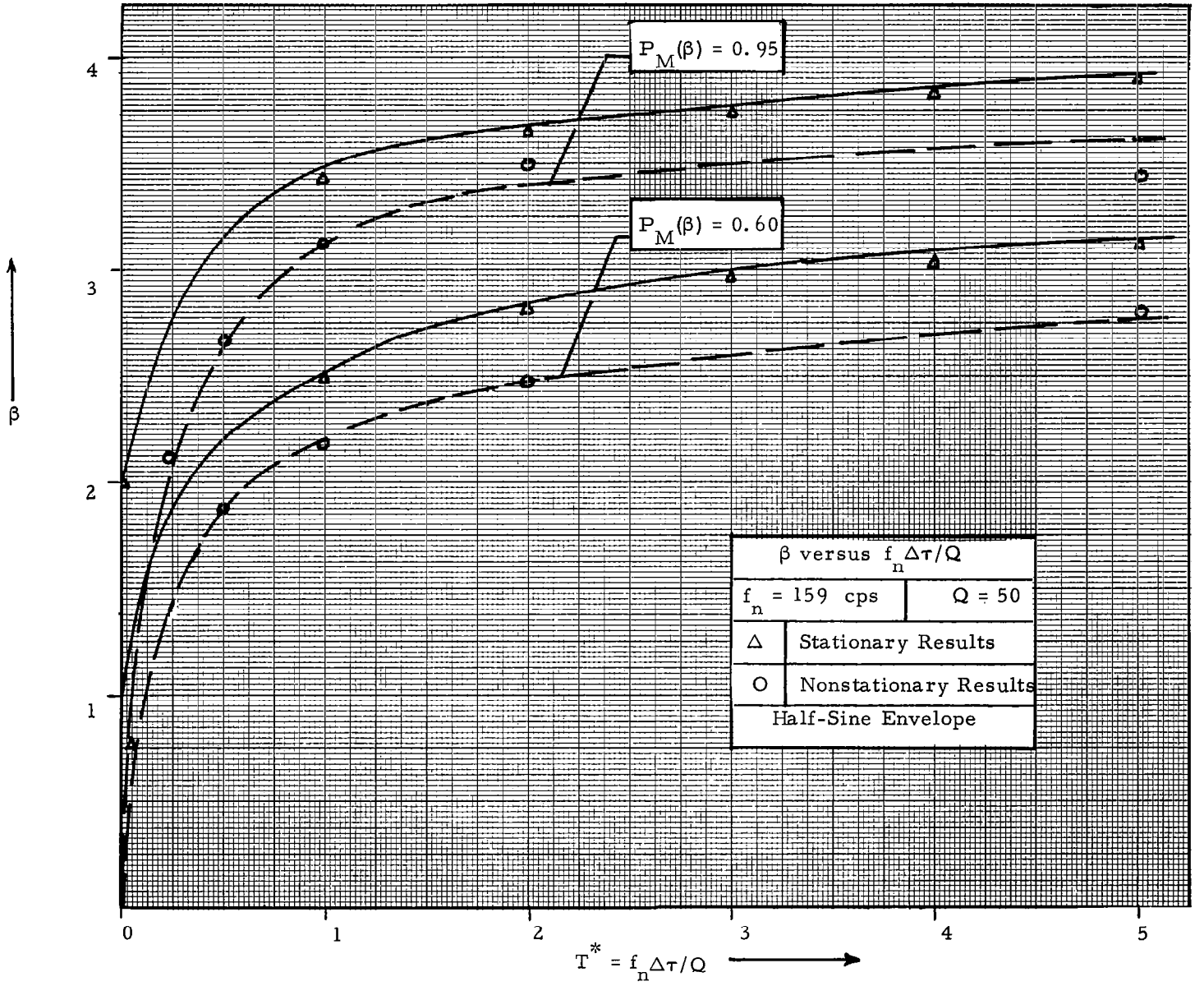

Figure 20. Ratio of Peak Response to RMS Response for the Mechanical Oscillator (β) Versus the Dimensionless Time Parameter (T*) for Stationary and Pulsed Random Excitation. Half-Sine Envelope, Q = 50

4. CONCLUDING REMARKS

4.1 SUMMARY

This report considers the peak response behavior of a linear mechanical oscillator when subjected to stationary and nonstationary random excitation. The peak response is expressed as a ratio of peak to rms response and is denoted as β. The stationary random excitation is white noise and the nonstationary random excitations are pulses of white noise shaped in time as either a rectangle or a half-sine. The peak response results were obtained by an analog computer study and are displayed as a family of constant probability curves with β plotted versus a dimensionless time parameter denoted as T^*. This parameter contains the undamped natural frequency of the oscillator (f_n), the damping of the oscillator expressed as Q, and a time duration noted as T for stationary white noise and $\Delta\tau$ for the shaped white noise.

The β results for stationary white noise are seen to establish an upper bound on the β results for the pulses of shaped white noise. Thus, the stationary white noise β plots can be applied to conservatively predict the peak response of an oscillator to pulsed random excitation. For T^* values < 1 (that is, the time duration of the pulse is relatively short as compared to the natural period of the oscillator), the β results for stationary white noise yield highly conservative estimates. For $T^* > 1$, the white noise β results, although still conservative, are more nearly the same order of magnitude as the β results for the shaped white noise. For a small number of response cycles, the peak to rms response ratio is noted to be dependent on the Q of the oscillator for each $P_M(\beta)$. For a larger number of response cycles, however, these peak to rms results tend to become independent of Q.

For the linear oscillator, the β curves provide an empirical answer to the following basic nontrivial questions which are of practical importance in mechanical design:

(1) How high an amplitude would be reached in a finite time interval T with probability $P_M(\beta)$? It is recalled that $P_M(\beta)$ is defined as the probability that M, the maximum value for the envelope peak in time T, is $\leq \beta$ times the rms response value.

(2) What length of time is necessary for an oscillator to effectively achieve stationarity in its response after being excited by a pulse of random excitation?

The first question arises in extreme value problems where one is concerned with the likelihood of a single catastrophic event. For example, what is the probability that some basic structure of an aircraft will experience an extreme stress beyond ultimate strength due to a gust load during its service life? For a second example, what is the probability that a resiliently mounted equipment package in a spacecraft will collide with neighboring structure due to random vibration during the launch phase? The second question arises in those cases where one is concerned with making stationary approximations for nonstationary environments. For example, will a stationary vibration test properly simulate the most severe response conditions which a component experiences during exposure to a nonstationary vibration environment.

Continuing with the example of vibration testing, assume the first crossing of a given extreme stress level will produce a failure of the component to be tested. Such a failure criterion is often acceptable for components subjected to intense, short duration vibration environments such as launch environments for space craft. As indicated by the β curves, the probability of a given extreme value is a function of both the rms value for the vibration and the exposure time. Hence, the β curves can be used as a criterion to arrive at appropriate test levels by specifying (1) the time varying rms magnitude of the environment, (2) an acceptable peak value probability, i.e., a $P_M(\beta)$ value, and (3) the expected time exposure in the random environment. From these data and the β curves, a stationary vibration test can be specified which simulates a nonstationary vibration environment.

The β curves depict in a general way the time-probabilistic behavior of the peak response of a linear oscillator excited by both stationary and nonstationary random excitation. These results, however, can be applied to provide qualified solutions to various specific problem areas such as for test specifications which are discussed briefly on the previous page. It must be understood that conclusions drawn from the β curves are based upon an extreme value criterion and can be applied to problems only where such a criterion is plausible.

4.2 RECOMMENDATIONS FOR FUTURE STUDIES

On the basis of this report, several important topic areas are recommended for future study. For the mechanical oscillator:

- Repeat the analog study for other values of f_n, Q, and T (or $\Delta\tau$) to establish response results which are statistically more significant.
- Consider envelope shape functions other than a rectangle or half-sine (for example, a triangle or a trapezoid).
- Consider the effects on the β parameter of varying the oscillator center frequency (f_n) over the frequency band of the input excitation where the input spectrum is other than white noise.
- Consider the effects of nonlinearities on the β parameter.

Similar studies also should be performed for multi degree-of-freedom systems to determine the significant parameters affecting the β response.

Although the above recommendations can be effectively carried out using electrical analog equipment (as in this report) an alternative program would be to perform the suggested analog experiments by digital or hybrid methods. In these ways, the vast amount of peak response data can be routinely and efficiently organized to form the desired $P_M(\beta)$ versus β plots as well as the β versus $f_n T/Q$ curves.

REFERENCES

1. Rice, S. C., "Mathematical Analysis of Random Noise," Selected Papers on Noise and Stochastic Processes, Dover Publications, 1954.

2. Crandall, S. H. and W. D. Mark, Random Vibration in Mechanical Systems, Academic Press, New York, 1963.

3. Enochson, L. D., "Frequency Response Functions and Coherence Functions for Multiple Input Linear Systems," NASA CR-32 (N64-17989), National Aeronautics and Space Administration, Washington, D. C., April 1964.

4. Barnoski, R. L., "Response of Elastic Structures to Deterministic and Random Excitation," AFFDL TR-64-199, Air Force Flight Dynamics Laboratory, Wright-Patterson Air Force Base, Ohio.

5. Piersol, A. G., "The Measurement and Interpretation of Ordinary Power Spectra for Vibration Problems," National Aeronautics and Space Administration, Washington, D. C., NASA CR-90, September 1964.

6. Clarkson, B. L., and R. D. Ford, "The Response of a typical Aircraft Structure to Jet Noise," Journal of the Royal Aeronautical Society, Vol. 66, No. 613, January 1962.

7. G. P. Thrall, and J. S. Bendat, "Mean and Mean Square Measurements of Nonstationary Random Processes," MAC 305-07.

8. Bendat, J. S. and G. P. Thrall, "Spectra of Nonstationary Random Processes," AFFDL TR-64-198, Research and Technology Division, AFSC, USAF, Wright-Patterson Air Force Base, Ohio, November 1964.

9. Bendat, J. S., Enochson, L. D., Klein, G. H., and A. G. Piersol, "The Advanced Concepts of Stochastic Processes and Statistics for Flight Vehicle Vibration Estimation and Measurement," ASD TR 62-973, Aeronautical Systems Division, AFSC, USAF, Wright-Patterson AFB, Ohio, December 1962. (AD 297 031)

10. Caughey, T. K. and H. J. Stumpf, "Transient Response of a Dynamic System under Random Excitation," Journal of Applied Mechanics, December 1961, pp.563-566.

11. Barnoski, R. L. and R. H. MacNeal, "An Investigation of the Maximum Response of a Single Degree of Freedom System Subjected to Stationary Random Noise," CEA Project No. ES 182-5, Technical Report prepared by Computer Engineering Associates, Pasadena, California for Lockheed Missile and Space Company, Sunnyvale, California, November 1961.

12. Barnoski, R. L. and R. H. MacNeal, "The Peak Response of Simple Mechanical Systems to Random Excitation," CEA Project No. ES 182-6. Technical Report prepared by Computer Engineering Associates, Pasadena, California, for Lockheed Missiles and Space Company, Sunnyvale, California, March 1962.

13. Lin, Y. K., "Nonstationary Response of Continuous to Random Loading," The Journal of the Acoustical Society of America, Vol. 35, No. 2, February 1963, pp. 222-227.

14. Aspinwall, D. M., "An Approximate Distribution for Maximum Response During a Random Vibration," Lockheed Missiles and Space Company, Report No. TM 53-16 MD-5, May 1961.

15. Thrall, G. P., "Extreme Values of Random Processes in Seakeeping Applications," MAC 307-03, Contract Nonr-4305(00), August 1964.